CHALMERS

Characterization of Pt/CeO_2 catalysts

Thermal ageing studies of high surface area support and evaluation of chemisorption based dispersion measurements

Master of Science Thesis

SUSANNE RYBERG

Department of Chemical and Biological Engineering
Applied Surface Chemistry / Competence Centre for Catalysis
CHALMERS UNIVERSITY OF TECHNOLOGY
Göteborg, Sweden, 2010

Thesis for the degree of Master of Science

Characterization of Pt/CeO_2 catalysts

Thermal ageing studies of high surface area support and evaluation of chemisorption based dispersion measurements

Susanne Ryberg

Department of Chemical and Biological Engineering
Applied Surface Chemistry / Competence Centre for Catalysis
CHALMERS UNIVERSITY OF TECHNOLOGY
Göteborg, Sweden, 2010

Characterization of Pt/CeO_2 catalysts
Thermal ageing studies of high surface area support and evaluation of chemisorption based dispersion measurements
SUSANNE RYBERG

Department of Chemical and Biological Engineering
Chalmers University of Technology
SE-412 96 Göteborg
Sweden
Telephone + 46 (0)31-772 1000

Cover:
[Honeycomb cordierite used for catalyst manufacturing, here cut in the shape of hearts and painted with acrylic colour.]

Göteborg, Sweden 2010

Characterization of Pt/CeO_2 catalysts

Thermal ageing studies of high surface area support and evaluation of chemisorption based dispersion measurements

SUSANNE RYBERG

Department of Chemical and Biological Engineering
Chalmers University of Technology

Abstract

For the future demands in the fields of catalysis, it is necessary to develop new highly active catalysts for removal of emissions from combustion of conventional as well as new bio-based fuels. Ceria has been shown to be an interesting support material for noble metals in catalysts designed for emission control, mainly due to its oxygen storage capacity. Unfortunately, the presence of ceria in the support will cause some difficulties with estimation of noble metal dispersion using traditional methods. It is thus desirable to develop new methods suitable for determination of noble metal dispersion in catalysts containing ceria.

In this master thesis work, two methods for determination of platinum dispersion were evaluated in a flow-reactor and with diffuse reflectance infrared Fourier transform spectroscopy, DRIFTS. Classical methods for catalyst characterization based temperature programmed desorption and CO oxidation were also performed to acquire more knowledge about the Pt/CeO_2 system and connect these catalyst properties to the dispersion of platinum. Additionally, the impact of different heat treatments on the specific surface area of ceria was investigated. In this thesis work ceria with a high surface area was used and the loading of platinum was 1 or 3 wt. %.

The catalyst studied showed a high activity for CO oxidation at low temperatures. Temperatures below 400°C did not reduce the surface area of the ceria significantly neither in oxidizing nor reducing environment. The two methods for dispersion measurement exhibited repeatability. However, according to complementary DRIFTS measurements, none of the evaluated methods gave sufficiently good results for accurate determination of platinum dispersion in the Pt/CeO_2 system.

Keywords: ceria, Diffuse reflectance infrared Fourier transform spectroscopy, dispersion, platinum, catalytic activity, catalyst characterization

Table of contents

List of abbreviations

BET	Brunauer, Emmett and Teller
CeO_2	ceria, cerium oxide
CO	carbon monoxide
cpsi	cells per square inch
DRIFT(S)	diffuse reflectance infrared Fourier transform spectroscopy
GHSV	gas hourly space velocity
HA	high specific surface area
IP	isoelectric point
LA	low specific surface area
MS	mass spectrometer
OSC	oxygen storage capacity
Pt	platinum
S	stabilization
SA	surface area
SSA	specific surface area
TPD	temperature programmed desorption

1. Introduction

Cerium oxide (CeO_2) commonly referred to as ceria, is an interesting support material in catalyst applications, one of the reasons being its oxygen storage ability. Ceria is currently used as a component in three-way catalysts to function as an oxygen buffer [1]. However, ceria might also be an interesting material in the new catalyst systems that have to be developed in order to meet future emission standards for automotives.

The high efficiency of modern engines leads to cold exhausts, well below 200°C for significant periods. The ordinary three-way catalyst cannot provide sufficient conversion under these conditions and thus, catalysts active at low temperature are required. Another aspect is that the use of biofuels put new demands on the emission treatment system. The catalyst must be able to convert emissions from these new fuels, with a high content of compounds that are difficult to convert at low temperatures, e.g. carbon monoxide (CO) and methane.

It has been shown in previous work that ceria supported platinum catalysts (Pt/CeO_2) are very active for oxidation of both CO [2] and methane [3]. However, the reason for this is not yet clear. In order to improve the design of this catalyst it is of interest to understand the operation mechanism behind this high activity as well as the basic characteristics of the systems.

Characterization of noble metal/ceria catalysts is unfortunately connected with some difficulties. Dispersion of the active material (e.g. platinum) is one of the most important characteristics of a catalyst and greatly influences the activity of the system. A large surface area per amount of material is usually desired. The dispersion is normally measured by chemisorption of a probe molecule (e.g. CO or H_2) that only adsorb onto the metal surface, not on the support material [4]. However, since ceria is a very active support material and also adsorbs the probe molecule these traditional methods are difficult to use [5, 6].

1.1 Aim

The aim of this master thesis project was to acquire more knowledge about the Pt/CeO_2 system. As a starting point for this study it was investigated how the structure of the ceria support is affected by temperature.

More importantly, methods for measurements of platinum dispersion of Pt/CeO_2 catalysts were evaluated. It is desired to find a method that does not destroy the sample to enable measurements before and after reactions. Finally the conversion of CO was studied in a flow reactor to connect the catalytic activity to the catalyst characteristics previously measured.

2. Theory

In order to understand the aim of this master thesis and the different methods used, some background in the field of catalysis is necessary. This chapter contains a short introduction to the concepts in the field of catalysis that are most essential in this work.

2.1 Catalysis

Catalysis is one of the most important technologies in our modern world. The majority of people are aware of the usage of catalysts to remove pollutants from the exhaust of car engines, but catalysts are used for so much more than emission control. A vast number of different catalysts are used in the conversion of crude oil, natural gas and coal into fuels and various bulk chemicals. They are used in production of plastic, fertilizer and pharmaceuticals. They can also be found in our own bodies, since all enzymes are proteins with a catalytic function [7].

A catalyst is a substance that accelerates the rate of a reaction, and while being intimately involved in the reaction sequence will not be consumed itself. It should be noticed that a catalyst cannot change the thermodynamics of a reaction, i.e. no thermodynamically impossible reaction can be made possible using a catalyst. It is only the reaction rate which is affected by a catalyst, not the equilibrium.

Catalysis can be divided into two general categories: heterogeneous and homogeneous catalysis.
Heterogeneous catalysis – the catalyst and the reactant are in different phases, e.g. oxidation of CO gas over a solid Pt/alumina catalyst.
Homogeneous catalysis – the catalyst and the reactant are in the same phase, e.g. ozone destruction catalyzed by Cl radical atoms in the atmosphere [8].
The reactions and mechanisms in this thesis work belonged to the former category, heterogeneous catalysis, and the rest of the theory chapter will focus on systems with gas phase reactants and solid catalyst.

2.1.1 The catalytic cycle and driving forces

The general process in heterogeneous catalysis involves a number of steps, as can be seen in the schematic description in figure 1. In the first step, the reactants diffuse through the gas phase and adsorb on the catalyst surface. The reactants may remain adsorbed as the original compound, i.e. molecular adsorption, or dissociate into fragments or atoms, i.e. dissociative adsorption. The reactants may diffuse on the surface before the reaction takes place. Finally the product desorbs and diffuses away from the surface into the gas phase.

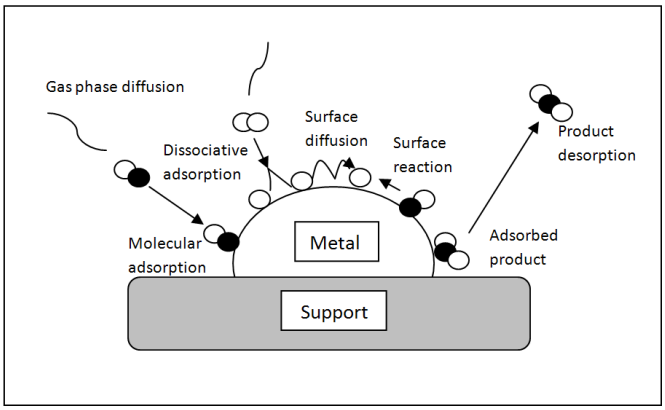

Figure 1: Molecular events (elementary steps) that may be involved in the catalytic cycle for a supported catalyst.

With the catalytic process in mind, it can clearly be understood that the surface structure is very important for the function of the catalyst. The very essence of the catalytic activity can be found in the atoms located at this interface. These atoms do not coordinate with neighboring atoms in the same manner as the bulk atoms. The abrupt termination of the structure leaves free bonds available for interaction with incoming atoms/molecules. Preferably, these incoming species will be the reactants in the reaction that is to be catalyzed and not other atoms that may adsorb and block the sites. In thermodynamic terms, the surface represents a high energy state and if possible it will be lowered by various mechanisms.

The available bonding sites provide an alternative pathway for the reaction. This pathway has lower activation energy barriers compared to the uncatalyzed reaction and this will enhance the rate of the overall reaction. In gas phase, a large amount of energy is required to break the old bonds and create intermediates with unsatisfied valences while on the surface, the stabilizing effect from the catalyst will reduce the energy needed. This is illustrated in figure 2, which also contains the energy barriers associated with the different steps in the catalytic process.

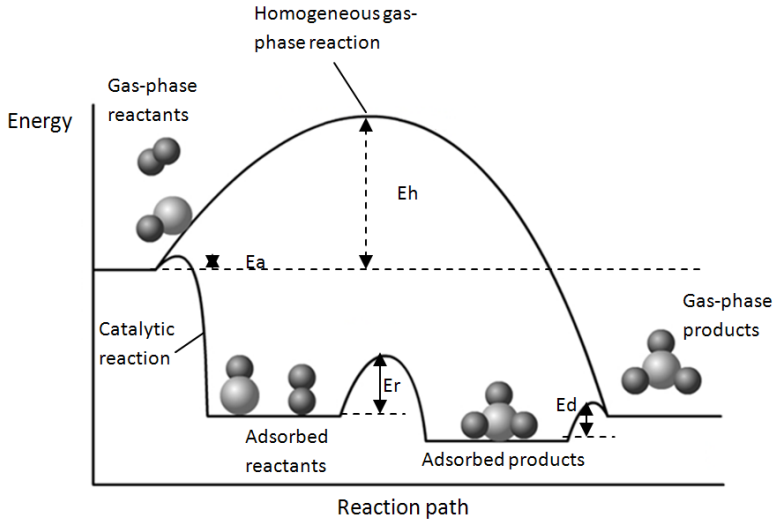

Figure2: Energy barriers involved in homogeneous uncatalyzed gas phase reactions and catalytic reactions. Eh = activation energy for the homogeneous gas phase reaction, Ea = activation energy for adsorption, Er = activation energy for the catalytic surface reaction, Ed = activation energy for desorption of products.

2.1.2 Surface properties

A large surface area is desired in most catalysts to provide many active sites, i.e. sites where reactions can take place. A property commonly used to describe catalytic materials is the specific surface area (SSA), which is the surface area given per mass, m^2g^{-1}. Supported catalysts can have SSA up to ca. 200 m^2/g [8]. Dispersion is another important property for catalysts. It is defined as the relationship between the number of surface atoms and the total number of atoms, usually given for the catalytically active component(s).

$$Dispersion(\%) = \frac{number\ of\ atoms\ at\ the\ surface}{number\ of\ total\ atoms} \cdot 100 \qquad \text{equation (1)}$$

A high dispersion means that many atoms are at the surface and implies an effective usage of the component. Dispersion can be calculated for a single substance, as well as for an entire system.

Not only does the amount of the available surface sites, but also the structure on the nanoscale level influence the activity. A surface is usually never flat on the atomic scale; the morphology may contain different facets, steps, missing atoms and various deviations and each of these sites have different affinity for adsorbing atoms due to their varying coordination number. A small addition of another compound may change the nature of the active sites and thereby change the catalytic properties, such as activity, selectivity or lifetime. If any of the mentioned properties is enhanced, the additive is called a promoter and if lowered, a poison [8].

2.1.3 Physisorption and chemisorption

The strength of adsorption may vary by several orders of magnitude. The weaker type of adsorption is referred to as physisorption and originates from Van der Waals forces and electrostatic polarization [8]. Strong interaction involves forces similar to those in ordinary chemical compounds and this phenomenon is called chemisorption. Chemisorption may also involve weakening or breaking of the internal bond in the adsorbing molecule and is usually favorable in catalysis. Using CO-oxidation on Pt as an example once again, O_2 preferably adsorbs dissociatively while CO does not, due to the much higher internal bond strength of CO (1076 kJ mol^{-1} for CO vs. 500 kJ mol^{-1} for O_2)[8]. The energy barriers between different adsorption states depend on the solid involved, its surface structure and the nature of the incoming molecule.

The high energy state of the free surface and its tendency to attract molecules from the gas phase as previously described is the driving force for catalysis, but this attraction can also be too strong to provide a good catalytic process. If the adsorbents bind too strong, they will not be released into the gas phase and the active sites will be blocked. The catalyst will be self-poisoned and its activity will be very low. Hence, in order to obtain a high reaction rate, the adsorbent should bind neither too weak nor too strong.

2.1.4 Deactivation and lifetime

In the definition of a catalyst, it is stated that the catalyst itself should not be consumed. Practically however, most catalysts have a limited lifetime. A number of mechanisms take place that will lower the activity and/or the selectivity of the catalyst and finally render it useless. The driving force behind these processes, as well as the catalytic activity, is lowering of the surface energy. The most common deactivation mechanisms will be described below.

Sintering, i.e. collapse of the structure and aggregation of particles cause loss of surface area and will significantly affect catalytic systems. Sintering is usually enhanced by increased temperatures and will decrease the activity. If the system consists of more than one component, different components may have different sensitivity towards sintering.

Another very common deactivation mechanism is poisoning, where a substance blocks active sites and/or electronically influence the surrounding sites in a negative way. This process may range from just a few blocked sites, to a completely covered surface and finally large depositions blocking the surface as well as pores in the material. The substance causing poisoning may be a substance not participating in the reaction or one of the reactants/product. An example of the later is the susceptibility towards CO of noble metals in ordinary catalytic converters at low temperatures. Before a sufficient temperature has been reached (i.e. the temperature for CO desorption) CO forms a very dense overlayer on the surface thus occupying/blocking the majority of the active sites. No other reactant can reach the surface and participate in a reaction and the catalytic converter remains inactive [9]. A poisoning process might be reversible, while sintering usually is irreversible.

A more physical way of decreasing the performance of a catalyst is attrition, where the catalyst material is crushed. This will block the reactor and reduce the gas flow, causing a decreased production. For a practical application, the activity alone is not the most important parameter but rather a combination of activity and lifetime.

2.1.5 Structure of commercial catalysts

Catalysts come in a broad range of forms, depending on the type of application. They are exposed to a number of environmental factors, such as elevated temperatures, high flow speeds and a harsh chemical surrounding. To avoid deactivation these factors should be considered in the system design.

In some applications, the active material is added directly to the reactants as a powder or pressed pellet. However, a common way to increase the activity, stability and lifetime of the catalyst is to deposit the active phase on a support material. The support should provide a high surface area as well as thermal and mechanical resistance. The tendency of active particles to aggregate is lowered if they are well separated and bound to a support compared to when being in direct contact. The support may be catalytically inert, but it may also contribute to the overall catalytic activity. Common support materials are silica, alumina and carbon.

If and unrestricted gas flow is important, pellets with an open design can be used, but a much more common approach is to use substrates, such as monoliths. The open honeycomb structure allows high gas flows. Some examples of different monolith structures can be seen in figure 3.

Figure 3: Various monoliths used in catalysis [10]

The active catalyst material and the support may be deposited at the same time on the monolith as will be described later in the report, or in two separate steps. The monolith design is used in most tree-way catalytic converters today, an example can be seen in figure 4.

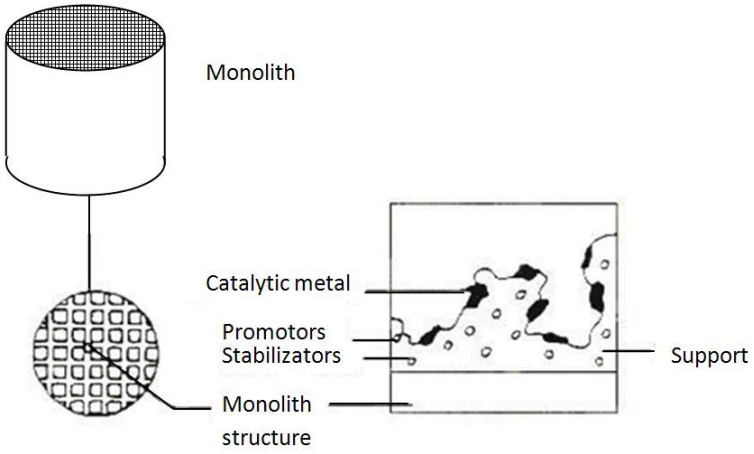

Figure 4: Monolith, support and active material in a catalytic system.

2.2 Catalyst characterization

Characterization of catalysts provides a number of challenges since the processes are taking place over wide length and time scales. Maybe the most accurate situation for evaluation of a catalyst is in an industrial application, but this is not suitable due to practical reasons. Reactors have to be scaled down for easier handling and different catalyst components may have to be studied separately to understand their function.

2.2.1 BET

The specific surface area (SSA) of a catalyst is usually determined using the BET method [7]. The method is based on physisorption of N_2 molecules. The N_2 molecules are allowed to physisorb on the surface at low temperature and will start to form a monolayer. Nitrogen molecules pack together independent of the atomic structure of the surface and one single N_2 molecule occupies 0.162 nm^2. The method is however not entirely straight-forward since multilayers may form in some areas before the monolayer still is being filled in others. But this is compensated for in the BET approach by

measuring at low absorbent pressures. A number of other restrictions must also be accepted, such as assumptions regarding lack of adsorbate-adsorbate interactions and equivalent adsorption sites.

The BET equation (derived by Brunauer, Emmett and Teller) is used to determine the monolayer volume, V_m which in turn will give the surface area, SA.
The BET equation [8]:

$$\frac{1}{V[(P_0/P)-1]} = \frac{C-1}{V_m}\left(\frac{P}{P_0}\right) + \frac{1}{V_m C} \qquad \text{equation (2)}$$

P	Equilibrium pressure for a particular surface coverage.
P_0	The saturated vapour pressure of the liquid adsorbate at the adsorption temperature.
V	The volumetric uptake of gas at pressure P.
C	constant

The experiment is performed at 77 K and the parameters that are measured is the amount of added gas, V and the pressure P. P_0 can be given by standard data but is usually measures by the instrument. A linear graph based on equation 2 is made with $1/(V[(P_0/P)-1])$ on the y-axis and P/P_0 on the x-axis. V_m is extracted from the slope and the intercept.

The surface area (SA) is then calculated with:

$$SA(m^2) = V_m \cdot N_A/V_A \cdot A \qquad \text{equation (3)}$$

N_A/V_A	Avogadro's number per unit volume of gas
A	Area of the adsorbate molecule (N_2)

To obtain the SSA (m^2/g), SA is divided by the weight of the sample. N_A/V_A should be given by standard data and the calculations described above can be automatically performed by the instrument.

The total surface area is important since a large area favours a good dispersion and large activity. But it should be stressed that N_2 adsorbs in a non-specific way and hence, measurements of the total surface area will not give any information about the dispersion of the active phase.

2.2.2 Measurements of dispersion

Methods based on specific chemisorption are useful for determining the number of surface atoms for a particular active component of a catalyst. If the mass of this component is known, the dispersion can also be calculated by using equation 1. Instead of N_2, which physisorb non-specific, a specie that is known to chemisorb specifically on the active component must be used. Common probe molecules are H_2, CO, O_2 and N_2O.

In this method, the active molecules are allowed to adsorb at low temperature. Then the reactor is flushed with inert gas (e.g. argon) in order to desorb the molecules that only are physisorbed. After this, two different approaches can be used:

1. A second pulse of active molecules is added. The difference between the amount of active gas in the outlet gas during the second pulse compared to the amount in the outlet gas during the first pulse, represents the number of molecules that are stuck on the surface, i.e. chemisorbed. A schematic illustration of this approach can be seen in figure 5.

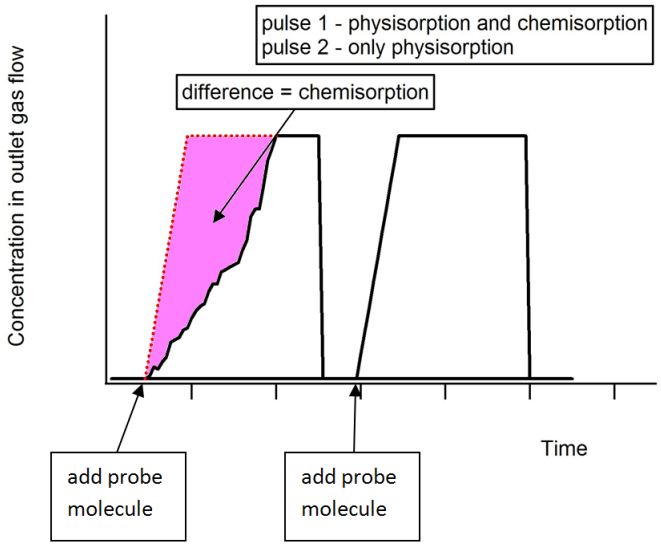

Figure 5: Measurements of chemisorbed molecules.

2. The sample is exposed to increased temperature under an inert gas flow. This method is called temperature programmed desorption (TPD). As the temperature is raised, the adsorbed molecules will desorb. The temperature where a molecule desorbs is correlated to the bonding strength. Desorption peaks at low temperatures usually originates from physisorbed molecules while the peaks at higher temperatures originates from chemisorbed ones.

In both these approaches, equipment able of quantitative measurements must be used to monitor the composition of the outlet gas flow. Also, some assumptions have to be made regarding the number surface atoms a probe molecule coordinates to. The total number of surface atoms is given by the chemisorbed probe molecules in approach 1 or 2 and the dispersion can be calculated according to equation 1.

Another method that could be used to measure dispersion is transmission electron microscopy (TEM). This approach is quite tedious since a lot of pictures must be acquired of different part of the structure before the dispersion of the active phase can be estimated. This method is also difficult to use on a system when both the active phase and the support contains atoms of high atomic number [11]. A high dispersion also causes problems with the contrast of the pictures.

2.2.3 Diffuse reflectance infrared Fourier transform spectroscopy

Fourier transform infrared spectroscopy (FTIR) in transmission mode has been used for many years to obtain qualitative and quantitative information from a wide variety of samples. Infrared spectroscopy is based on ability of molecules to absorb light in the infrared region (4000-200 cm^{-1})

[12] by excitations in the vibrational and/or rotational mode. The energy of infrared light is too low to excite electron states. A large advantage with IR is that it can be used *in situ* to monitor chemical processes. However, the method only works on molecules that are IR active, i.e. posses a change in dipole moment during the vibration. The intensity of the infrared band is proportional to the change in dipole moment, but it is sufficient that the dipole moment changes, a permanent dipole is not necessary. Hence, molecules with polar bonds like CO, NO and OH show strong IR absorption bands while species containing the more covalent C-C and N=N bonds show weaker bands. Species like N_2 and H_2, with non-polar bonds are not IR-active at all [13].

The use of the interferometer and the mathematical method of Fourier transform have enabled faster measurements since all wavelengths can be measured in a single run and FTIR has now to a large extent replaced traditional IR-methods.

A major drawback with FTIR in transmission mode is that it is not suitable for opaque materials or surface analysis. For these measurements, diffuse reflectance infrared Fourier transform spectroscopy (DRIFTS) is more suitable [14]. In DRIFTS, the IR beam is directed toward the sample at an angle and the IR radiation is reflected with many internal reflections in the sample before leaving in all directions. Part of the reflected radiation is collected by an ellipsoidal mirror and directed to the detector. With this approach, it is never necessary for the beam to pass straight through the sample.

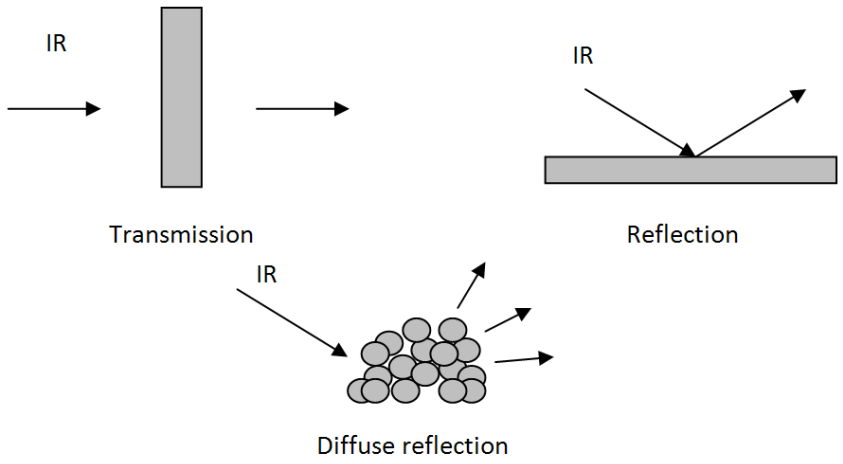

Figure 6: Different modes typically used in IR spectroscopy.

The sample preparation is very fast for DRIFTS experiments, a small sample cup is immediately filled with the powder sample. The sample may sometimes be diluted in a nonabsorbent powdered material. Due to the many internal reflections, quantitative information can be difficult to obtain, this is certainly a drawback with the DRIFT spectroscopy. For IR spectroscopy, each chemical bond is associated with a characteristic IR frequency. However, this frequency is also affected by the chemical surrounding, e.g. a change of support material will shift the signal from a certain adsorbate.

DRIFT spectroscopy is commonly used in the field of catalysis to identify adsorbed species and monitor how they change as a reaction proceeds. A convenient way of acquiring spectra which only show the adsorbing species is by subtracting a background spectrum from the spectra recorded during reaction. The background spectrum is recorded before exposure.

2.3 Characterization of catalysts containing ceria

Cerium is one of the rare earth metals and has two stable valences: Ce(IV) and Ce(III). Cerium easily forms cerium oxide, ceria in the range Ce_2O_3 – CeO_2. The final stoichiometry is strongly dependent on temperature and oxygen pressure [15]. Pure stoichiometric CeO_2 crystallises in the fluorite-structure, i.e. a face centred cubic unit cell with space group Fm3m. It is pale yellow in colour probably due to Ce(IV)–O(-II) charge transfer. Ceria tolerates a considerable reduction and the main compensating defects in CeO_{2-x} are oxygen vacancies. Reduced ceria turns blue and almost black when grossly nonstoichiometric [16]. The reduction is perfectly reversible and that is the reason behind the oxygen storage capacity (OSC) which this material exhibits [17]. Ceria form a number of different phases in the range Ce_2O_3 – CeO_2 which can be seen in figure 7. These phases show different structures, such as a disordered non-stoichiometric fluorite-related oxide (α-phase), highly ordered fluorite-related superstructures and even body-centred cubic (δ-phase) [15].

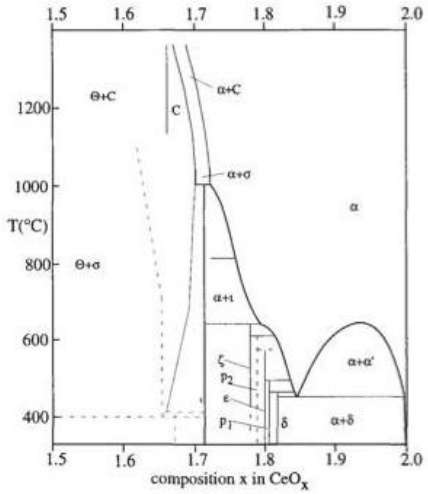

Figure 7: Phase diagram of ceria. [15]

Cerium oxide based ceramics are used in various applications, such as superconductors [18], gas sensors [19] and catalytic materials [15]. The OSC is the main reason for its usage as a component in catalyst support materials and is useful to achieve a high conversion of reactants. An example is adjustment of available oxygen during fluctuating air/fuel ratio in conversion of CO, NO_x and hydrocarbons over a three-way catalytic converter. Due to the high temperatures that may arise, ceria used in this application is commonly combined with other materials to obtain better refractory properties [20].

Ceria is certainly an important component in catalytic systems but unfortunately some difficulties arise during characterization of these systems. Dispersion of the active phase (Pt, Pd and Rh in a catalytic converter) is a crucial parameter for the activity and is commonly evaluated by chemisorption-based methods using H_2 and CO as probe molecules [4]. It is well known that the presence of ceria in a system will cause problems with the estimation of metal dispersion by these chemisorption-based methods. Spillover of probe molecules to the support easily occurs when H_2 [6] or CO [5] is used as probe, resulting in large errors in the dispersion values.

A number of different methods have been suggested to overcome the difficulties with measurement of metal dispersion in systems containing ceria. Chemisorption at low temperatures has been

investigated by several groups, both with H_2 and CO as probe molecule [21 - 24, 5]. Chemisorption with H_2 has also been evaluated at low pressures [22]. The aim with these approaches is to prevent the spill-over process. Chemisorption based methods where blocking of the ceria is utilized have also been suggested and will be described in detail in section 3.6.1 [5, 25]. After the ceria has been blocked, CO can be used as a probe molecule on Pt in a similar was as in ordinary chemisorption based methods.

A method utilizing DRIFTS has also been proposed. Papavasiliou et al. [26] have evaluated a method were a calibration curve was produced by acquiring the IR spectra of CO adsorbed at room temperature over a series of well characterized 0.5 wt.% Pt/Al_2O_3 catalysts. The acquired calibration curve was applied on a Pt/ceria-system. Duplan et al. [27] investigates the same approach in a system containing Pd instead of Pt.

The use of structurally insensitive reactions has also been evaluates for estimation of metal dispersion. Pantu et al. [28] employ propylene hydrogenation, a structurally insensitive reaction on both the alumina and the ceria supported metal catalyst. A relationship was established between the dispersion and the reaction rate on an Al_2O_3 supported catalyst. The values obtained were used to estimate the metal dispersion on the ceria supported catalyst. Rogemond et al. [29] employed a similar approach using cyclohexane instead.

By relating the parameter ΔI from the difference between the height of the white-line peaks in the L_3-edge in the XAS spectrum (fluorescence mode) to the size of the Pt particles, Nagai et al. [30, 31] can monitor the dispersion behaviour in real-time for a system with ceria-based support. The dispersion is not acquired in percent, but the size of the Pt particles is certainly related to their dispersion.

3. Materials and Methods

This chapter describes the materials and methods used in this thesis work. Some detailed information is also given about the equipment.

3.1 Materials

High surface area ceria-powder (99.5 H.S.A 514, Rhône-Poulenc)
13.82 wt.-% $Pt(NO_3)_2$ solution from Heraeus
20 wt.-% ceria-acetate sol from Nyacol Nano Technologies
Monoliths were cut from a commercial cordierite honeycomb wafer, 400 cpsi

3.2 Heat treatment of ceria powder

Heat treatment of ceria powder was performed to evaluate the influence of temperature, time and atmosphere on sintering. Treatments in oxidizing (air) atmosphere were performed in a Thermodyne SYBRON type 48000 furnace according to table 1. The samples were put into the furnace when it had reached the desired temperature and was immediately removed after the set time (±2 min).

Table 1: Heat treatment of ceria in oxidizing atmosphere.

Time [h]	Temperature [°C]											
2	250	300	350	400	450	500	550	600	650	700	750	800
17			350			500			650			800

Heat treatments of ceria samples were also performed in a reducing atmosphere, see table 2. To be able to provide this condition, a flow reactor (see section 3.5) was used instead of an ordinary furnace. Due to the construction of the equipment, the samples had to be kept inside the tube as it was heated to the desired temperature as well as cooled after set time. The tube was heated at 20°C/min in 100 ml/min argon flow until the desired temperature was achieved. After a few minutes for stabilization the composition of the gas flow was changed to 4 vol.-% H_2 in argon. After the 3 hours the temperature was lowered in argon before the sample was removed.

Table 2: Heat treatment of ceria in reducing atmosphere.

Time [h]	Temperature [°C]		
3	300	400	500

After heat-treatment, BET-measurements were performed on all samples to investigate temperature stability. The equipment used was a Micromeritics TriStar 3000 utilizing N_2 physisorption. The powders were heated for 2 h at 215 °C in a Heraeus type VT5042EK vacuum furnace before measurement to ensure that they were water-free.

3.3 Preparation of Pt/ceria-powder samples

Two different temperature-treatments were performed on ceria powder in order to obtain two clean powders with different specific surface areas. Suitable temperatures were based on the previous temperature study. The temperatures were chosen to 400°C and 800°C in air for 2 h to obtain samples with high respectively low surface area. Three different Pt/ceria powders were prepared, according to table 3:

Table 3: Composition of Pt/ceria powder samples.

High area ceria	Low area ceria
1 wt.-% Pt	1 wt.-% Pt
3 wt.-% Pt	

The Pt loadings were chosen as described in order to correspond to the expected difference in specific surface area between the high area (HA) and low area (LA) ceria powders. The HA sample was expected to have roughly three times larger specific surface area compared to the LA sample. Therefore, the HA + 3 wt.-% Pt sample (HA3) and the LA + 1 wt.-% Pt sample (LA1) were assumed to have the same ratio between Pt content and surface area and hence similar Pt species. The HA + 1 wt.-% Pt (HA1) and LA + 1 wt.-% Pt (LA1) samples would have the same Pt content in order to evaluate the influence of the specific surface area of the support on activity and storage.

For the Pt/ceria sample preparation, a Pt-nitrate solution (13.82 wt.-% Pt) was used as Pt precursor according to the table 4. In order to prepare 3 g of each powder sample, 217 or 651 mg of the platinum solution was used for samples with 1 or 3 wt.-% Pt.

Table 4: Calculations for Pt solution for catalyst synthesis.

Pt-content [%]	Mass Pt [mg]	Mass $PtNO_3$ solution [mg]
1	30	$\frac{30}{13.82} \cdot 100 = 217$
3	90	$\frac{90}{13.82} \cdot 100 = 651$

Ceria powder was impregnated with Pt –nitrate solution according to the incipient wetness method. The principle of this method is to add only as much liquid as the powder can hold before becoming "wetted". In this method, the noble metal precursor is forced to come close to the surface which facilitates high interaction [31]. If too much liquid (e.g. water) is used, the metal particles can move in the mixture and aggregate as the water slowly evaporates. Aggregation will give a lower dispersion and influence the activity of the catalyst in a negative way.

To achieve high interaction between the metal precursor and the support it is important to control pH. Opposite charges of the surface and the metal ion will favour adsorption while similar charges will prevent it. It has previously been shown that Pt-nitrate is a suitable precursor for impregnating positively charged surfaces [33].

To ensure that the surface was positively charged pH was kept well below the isoelectric point (IP) of the support material. The IP of ceria is approximately 7. This is close to the IP of alumina (Al_2O_3), a similar support material. It is known that alumina dissolve at low pH values and it can be suspected that ceria will behave in a similar fashion [34]. To keep a balance between dissolution of ceria and the number of positively charged surface sites, pH should preferably be around 3 during impregnation.

During the impregnation, the first step was to determine the amount of water the ceria powder samples could take up. It was found that 3 g HA ceria could absorb 1.4 g water whereas 3 g LA ceria only could absorb 1.2 g water.

The desired mass of Pt-nitrate solution was added to a small beaker and diluted with milliQ water. The pH was measured in one of the solutions using a pH indicator stick and was found to be between 2 and 3. Three grams of heat-treated ceria powder (LA or HA) was added to the beaker and the liquid and the powder was carefully mixed with a spatula for 10 minutes. The mixtures were frozen in liquid N_2, freeze-dried over night and finally calcined at 550°C for 15 min with a heating-ramp at 4.375°C/min from 25°C to 550°C. Freeze-drying was chosen because this method prevents aggregation of metal particles since the migration in liquid is suppressed. The water is immediately frozen and subsequently sublimates due to a supplied vacuum, preventing the formation of a liquid phase. Also, this treatment is considered less harmful to the support material.

In order to study the effect of the powder preparation on the specific surface area, BET measurements were performed on the HA1, LA1 and HA3 samples. Also, some HA1 powder was subjected to an elevated temperature in the flow-reactor in reducing environment, (400°C, 4 vol.-% H_2, 3 h) to investigate if Pt/ceria powder is more sensitive towards this treatment compared to pure ceria (section 3.2).

3.4 Preparation of monolith samples

The monoliths were cut to a 69-channel cylinder-shape from a 400 cpsi cordierite block of 2.0 cm thickness. Before being coated with catalyst material, the monoliths were calcined at 600°C for 1 h to remove any contamination.

In order to deposit active catalyst material on the monoliths they were immersed in a slurry containing Pt/ceria powder, ceria-acetate sol and milliQ water. The function of the ceria-acetate sol is to act as “glue” between the powder sample and the monolith. The ceria-acetate will decompose when heated, leaving a porous, but still stable Pt/ceria deposition on the monolith frame.

Approximately 200 mg dry material was desired on each monolith and for each batch a 50% excess was prepared, which gives a total of 300 mg per batch. The slurry contained 20 wt.-% dry material (Pt/ceria powder + ceria-acetate from sol) and 80 wt.-% water (water from sol + added milliQ water). One batch was prepared for each monolith in order to enable good mixing and correct deposition on the monolith. The final recipe for a slurry batch can be seen in the following table:

Table 5: Slurry recipe.

Component	Mass [mg]
Pt/ceria	240
ceria-acetate sol (20 wt.-% ceria)	300
milliQ water	960

The following procedure was utilized for impregnation of the monoliths:

1. The batch components were carefully mixed using a metal stirrer in a small beaker.
2. The weight of the empty monolith was noted.
3. Before dipping the monolith in the slurry for the first time, the monolith was dipped in milliQ water. The excess water in the channels was removed with pressurized air.
4. The monolith was immersed into the slurry a couple of time and shaken to remove excess liquid in the channels.
5. Dried with hot air gun at 90°C/5 min to remove water.

6. Dried with hot air gun at 600°C/2min to remove acetate.
7. Cooled with pressurized air and measure the weight.
8. Step 4-6 were repeated until approximately 200 mg material had been deposited on the monolith.

A final calcination was made at 400°C for 2 hours in the Thermodyne or Nabertherm furnace previously mentioned. Three different types of monoliths were made, using the three catalyst powders described in 3.3: HA ceria + 1 wt.-% Pt (HA1), LA ceria + 1 wt.-% Pt (LA1) and HA ceria + 3 wt.-% Pt (HA3).

The monoliths were characterized by BET to obtain their surface area both before and after their use in the flow reactor. Equipment suitable for monolith samples, a Micrometrics ASAP 2010 was used for this purpose.

3.5 Flow-reactor configuration

The flow reactor set-up can be seen in figure 8. Gases can be injected into the reactor using individual mass flow controllers connected to a computer. Up to five different gases can be used simultaneously in this equipment. The reactor chamber consists of a quartz tube surrounded by a metal coil for resistive heating. Two thermocouples are used to monitor the temperature of the gas and the monolith sample inside the reactor. These temperatures may differ, since the reactions taking place in the sample can give a different temperature inside the sample compared to the gas temperature. The thermocouple measuring the inlet gas temperature is connected to a Eurotherm regulator for control of the inlet gas temperature. The placement of the thermocouples is important in order achieve a similar temperature profile between different measurements.

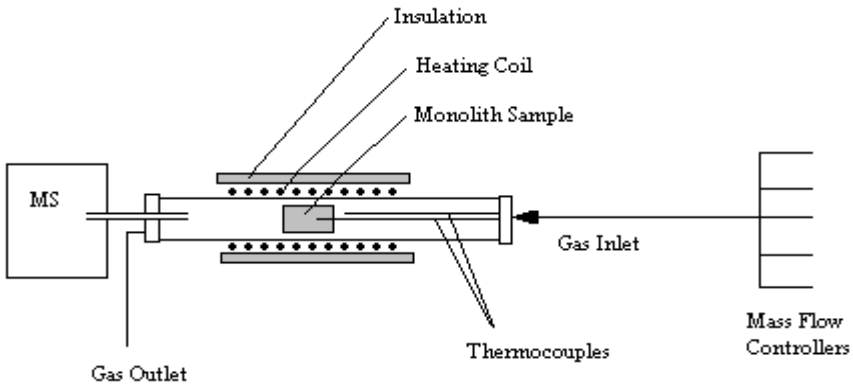

Figure 8: Flow-reactor configuration.

A mass spectrometer (MS), BalzersQuadstar 422, is used to monitor the composition of the outlet gas flow. A small portion of the total gas flow is entering the MS through the small quartz capillary while the majority is vented.

With a MS analytes can be measured both qualitative and quantitatively. The general principle is that the molecules are separated by their mass-to-charge ratios by the use of magnetic and/or electric fields. Before separation, uncharged molecules must be ionised by some method. Many molecules crack during ionisation and this cracking, or fragmentation, has to be accounted for when analysing a spectrum. A MS consist of an ion source which ionize the sample, a mass analyser that separate the

molecules/fragments and a detector as can be seen in figure 9. The detector usually consists of an ion/electron multiplier that monitors the incoming ions [35]. The signal from the MS is hence given as an ion current [A]. Different compounds give rise to different amounts of ions. Hence, a stronger signal from a certain compound need not imply this compound is present at a higher concentration compared to other compounds.

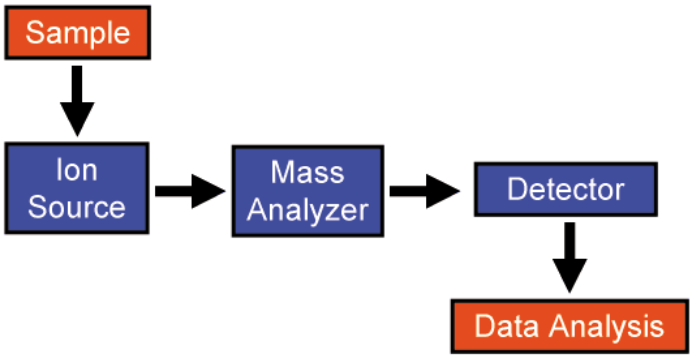

Figure 9: Main parts of a mass spectrometer [36].

In order to obtain quantitative data, a calibration measurement has to be performed where a known volume fraction of each gas is fed to the MS and the corresponding ion current is recorded. By measuring at different concentrations, a correlation between ion current and volume fraction can be obtained. This has to be done for each type of gas considered interesting. In this study it was done for CO_2, CO and methane.

The ion current signal also varies with the amount of gas that is able to enter to MS chamber through the capillary. A pressure meter shows the pressure inside the MS chamber and this corresponds to the amount of gas entering since a vacuum system prevents other materials from entering. A calibration is only valid at a given MS chamber pressure, i.e. for a certain capillary and it´s condition. The pressure may vary during a set of experiment if dust from the sample partially clogs the capillary.

3.6 Flow-reactor experiments

A series of flow reactor experiments, i.e. CO/H_2/CO, CO_2-poison, CO-TPD and CO oxidation, were performed with each of the monolith samples described in section 3.4. After the first set of runs, the monolith samples were aged for 2h in the reactor at 800°C (20 vol.-% O_2 in Ar) and the series of experiments was repeated on these “new” samples. This procedure results in six different samples. A summary of the different samples can be seen in table 6. Unless otherwise stated, the total flow was 400 ml/min
(GHSV=10600 h^{-1}) for the flow reactor experiments and Ar was used as balance.

Table 6: Sample matrix for TPD reactor experiments.

HA1 (monolith)	HA1 aged (monolith)
LA1 (monolith)	LA1 aged (monolith)
HA3 (monolith)	HA3 aged (monolith)

The aim of using this combination of methods was to both characterize the catalyst with conventional methods (e.g. TPD, CO oxidation) and to evaluate new methods for measurement of

the Pt dispersion. The experiments were repeated after ageing of the monolith samples to study the influence of support versus noble metal rearrangement.

Prior to each flow-reactor experiment, except for ageing and TPD experiments, a pre-treatment was performed to remove any contaminants. The pre-treatment consisted of an O_2-step (5 vol.-%) followed by a H_2-step (5 vol.-%) at 400°C. The duration of each step was 20 min.

The specific surface area of the monoliths before and after measurements in the flow reactor was measured with BET.

3.6.1 Methods for determination of noble metal dispersion

Two different methods for determination of noble metal dispersion were evaluated. Both methods contain a few steps that aim to cover ceria with C-containing species while keeping the Pt surface clean. After these initial steps, CO can be used as a probe molecule on Pt in a similar way as in ordinary chemisorption based methods.

In the first approach, a CO-pulse is combined with a reduction step in order to obtain a clean Pt-surface while keeping the ceria surface covered with CO [5]. In the last part of the method, CO can be used as a probe since only the Pt surface should be available. This method will be referred to as the $CO/H_2/CO$-method.

The second method utilize a CO_2-pulse that in combination with oxidizing and reducing steps only should cover the ceria, i.e. poison the ceria [25]. Subsequently, CO can be used as a probe on the Pt surface. This method will be referred to as the CO_2-poison method.

Graphic illustration of these methods can be seen in figure 10 and 11. Full scripts can be found in the appendix. To obtain more reliable results, each method was repeated twice on each of the six monolith samples.

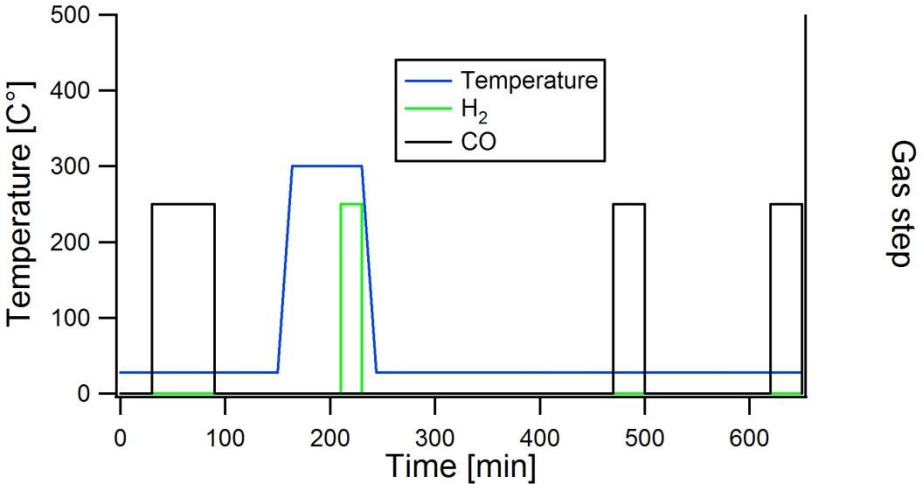

Figure 10: Graphic illustration of the $CO/H_2/CO$-method. Flow rate: 400 ml/min. Temperature gradient: 20°C/min, H_2-step concentration: 5 vol.-%, CO- step concentration: 150 ppm. Adsorption of CO at 28°C.

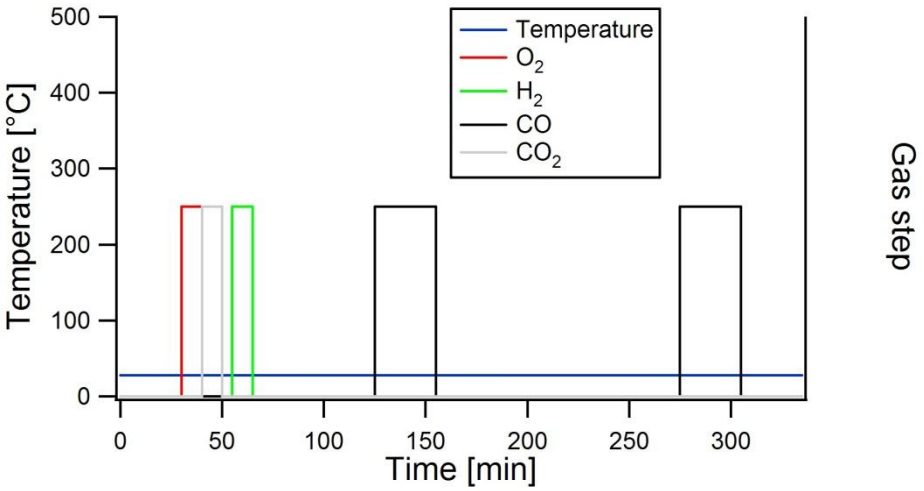

Figure 11: Graphic illustration of the CO_2-poison method. Flow rate: 400 ml/min. O_2-step concentration: 5 vol.-%, H_2-step concentration: 5 vol.-%, CO- step concentration: 150 ppm, CO_2-step concentration: 25 vol.-%. Adsorption of CO at 28°C.

The dispersion was calculated using the difference between the two last CO-steps. For the CO/H_2/CO method this meant CO step number 2 and 3, while for the CO_2-poison method CO step number 1 and 2.

In the second-last pulse, CO chemisorbs on Pt and physisorbs on the rest of the system (e.g. reactor walls). In the last pulse, the Pt surface is covered and only the system response is gained. Hence, the difference between the two last steps should correspond to the amount of CO chemisorbed on Pt. In this study, it is assumed for convenience that each CO molecule adsorbs linearly on one surface Pt atom, i.e. the stoichiometry is 1:1.

The volume fraction of CO in the reactor outlet flow during the CO-steps was calculated from the MS signal using a calibration file. The volume fraction versus time was integrated and multiplied with the flow to obtain the volume of CO gas in each pulse. The corresponding amount of moles was calculated using the ideal gas law and the difference between the two last pulses was calculated. The obtained amount of moles CO was assumed to correspond to an equal amount of available Pt on the surface and the dispersion could now be calculated according to equation 1.

3.6.2 Temperature programmed desorption

During a temperature programmed desorption (TPD) experiment the sample is heated and the different compounds emitted from the material are monitored. Information can be obtained about what kind of compounds that are adsorbed on the surface and the temperature at which they desorb is correlated to the strength of the interaction with the surface [37]. The TPD method can be performed under different conditions and an inert atmosphere was chosen in this work. The experiment was performed immediately after a CO/H_2/CO-experiment because it can be assumed that the whole surface is covered with CO-containing species after this treatment. The TPD experiment was only performed once on each monolith sample. The script for this method can be found in table 7.

Table 7. Script for TPD.

Temp. [°C]	Grad. [°C/min]	Duration [min]	Total flow [ml/min]	Comment
28	-	120	50	
28-800	20	39	50	Ar + heating
800	-	20	50	
800-28	20	39	50	
28	-	30	50	

3.6.3 Test of catalytic activity - CO oxidation

Oxidation of CO was performed to evaluate the catalytic activity of each sample. After the initial cleaning steps, CO and O_2 were introduced to the reactor at 300°C. The temperature was decreased to investigate at which temperature the activity was quenched. Finally, the temperature was raised again to investigate at which temperature the catalyst regained activity. These two parts of the method will be referred to as the extinction and ignition part. Oxidation of CO was only performed once on each monolith sample.

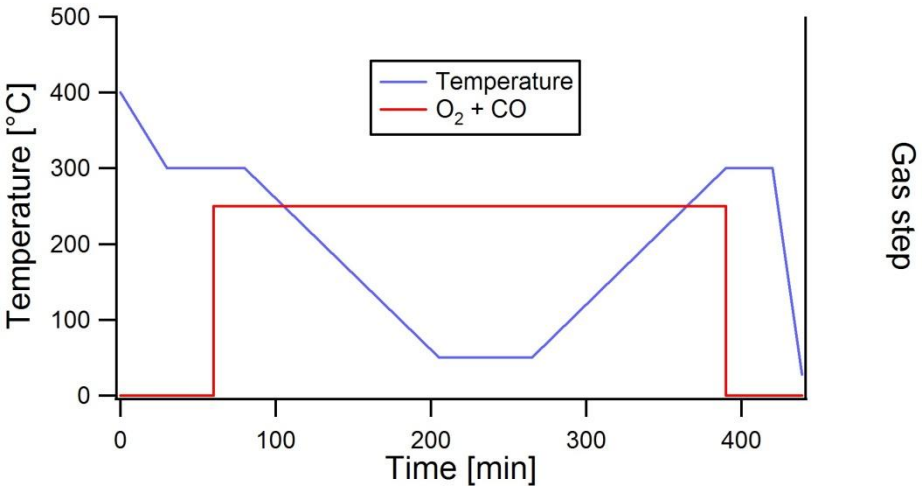

Figure 12: Graphic illustration of CO oxidation. Flow rate: 400 ml/min. Temperature gradient: 2°C/min, O_2/CO-step concentrations: 5 vol.-% O_2 and 0,5 vol.-% CO.

3.7 Diffuse reflectance infrared Fourier transform spectroscopy

To gain better understanding about the processes taking place on the sample surface during each individual step in the new methods for dispersion measurement, DRIFTS was used to monitor the surface species.

The set-up consists of a board of mass flow controllers and a Bio-Rad FTS6000 equipped with a Harrick Praying Mantis DRIFT cell that enable connection to a gas flow and controlled heating. An MS (BalzersQuadstar 422) is used to monitor the gases in the outflow. The reactor chamber is supplied with water cooling, which enables faster cooling steps. A fast switching valve (Vici Valco) can be used to rapidly switch between two different gases without interfering concentration gradients.

The same gases used in the TPD flow reactor can also be used in the DRIFTS equipment, so the $CO/H_2/CO$ and CO_2-poison methods described in 3.6.1 were rewritten for this set-up. The gas flow had to be lowered to 200 ml/min and some steps could be shortened due to the use of a switching valve. The complete scripts can be found in the appendix. It should be noted that only powder samples can be used in this equipment.

The $CO/H_2/CO$ experiment was performed on two different powders, HA1 and LA1 from the same batches which were used for preparing the monoliths. After the run on the HA1 powder, the pre-treatment steps of the method (described in section 3.6) was repeated to evaluate if the pre-treatment was able to clean a sample that already had been used. This was done to evaluate if the pre-treatment was suitable for repeated experiments. The CO_2-poison method was only investigated on one sample, HA1 powder.

All spectra were recorded in the range 4000-800 cm^{-1} with time resolution 1 or 2 s^{-1}.

4. Results

The following chapter contains the results obtained from the temperature study performed on ceria as well as from the flow reactor and DRIFTS experiments.

4.1 Influence of heat treatment on total surface area

Figure 13 shows the specific surface area of the high area ceria powder samples after treatments under different temperature, time and atmosphere.

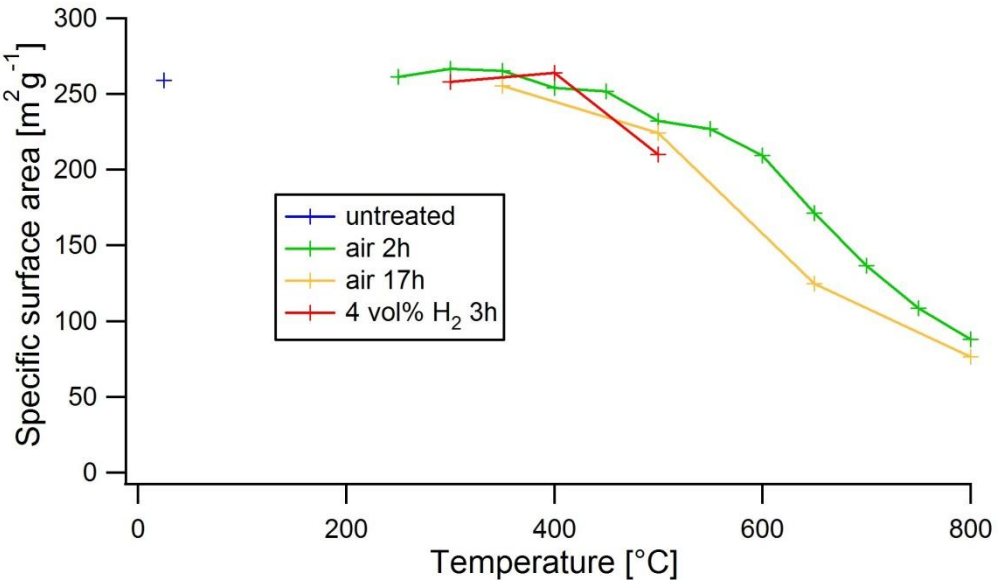

Figure 13: BET-area of ceria powder subjected to heat treatments.

As can be seen, the temperature must exceed 500°C to significantly influence the specific surface area of the ceria. Below this temperature, the BET surface area is in the range 200-250 m^2/g while for example at 650°C the BET surface area has decreased to approximately 140 m^2/g. The duration of the heat treatment has only a minor effect on the specific surface area. At the conditions use here, no significant difference between oxidizing and reducing atmosphere can be observed. It should be noted, however, that the ceria treated in a reducing atmosphere at 400 and 500°C changed colour from the original pale yellow to dark orange with some regions almost black.

A heat treatment in reducing atmosphere (400°C, 4 vol% H_2 for 3h) had also been performed on a HA1 powder sample. The SSA after this treatment was 186 m^2/g compared to 180 m^2/g before treatment.

4.2 Flow reactor experiments

4.2.1 Methods for determination of noble metal dispersion

The calculated dispersion from the two evaluated methods: $CO/H_2/CO$ and CO_2-posion can be seen in table 8. The dispersion was calculated assuming a 1:1 stoichiometry between adsorbed CO molecules and Pt surface atoms.

Table 8: Calculated dispersion obtained from $CO/H_2/CO$ and CO_2-posion methods.

HA1 (monolith)	Dispersion	LA1 (monolith)	Dispersion	HA3 (monolith)	Dispersion
$CO/H_2/CO$ (300ppm)	0,32	$CO/H_2/CO$	0,14	$CO/H_2/CO$	0,35
$CO/H_2/CO$	0,25	$CO/H_2/CO$	0,12	$CO/H_2/CO$	0,30
CO_2-poison	-	CO_2-poison	0,24	CO_2-poison	0,28
CO_2-poison	-	CO_2-poison	0,24	CO_2-poison	0,23
HA1 aged (monolith)	**Dispersion**	**LA1 aged (monolith)**	**Dispersion**	**HA3 aged (monolith)**	**Dispersion**
$CO/H_2/CO$	0,14	$CO/H_2/CO$	0,38	$CO/H_2/CO$	0,10
$CO/H_2/CO$	0,15	$CO/H_2/CO$	0,32	$CO/H_2/CO$	0,11
CO_2-poison	-	CO_2-poison	0,30	CO_2-poison	0,02
CO_2-poison	0,21	CO_2-poison	0,28	CO_2-poison	0,02

4.2.2 Temperature programmed desorption of carbon monoxide

The masses for H_2, CO, CO_2, O_2, methane and water were monitored during the TPD. No significant desorption peaks was observed for CO, O_2, methane or water and hence, only desorption graphs for H_2 and CO_2 are reported here, see figure 14 and 15.

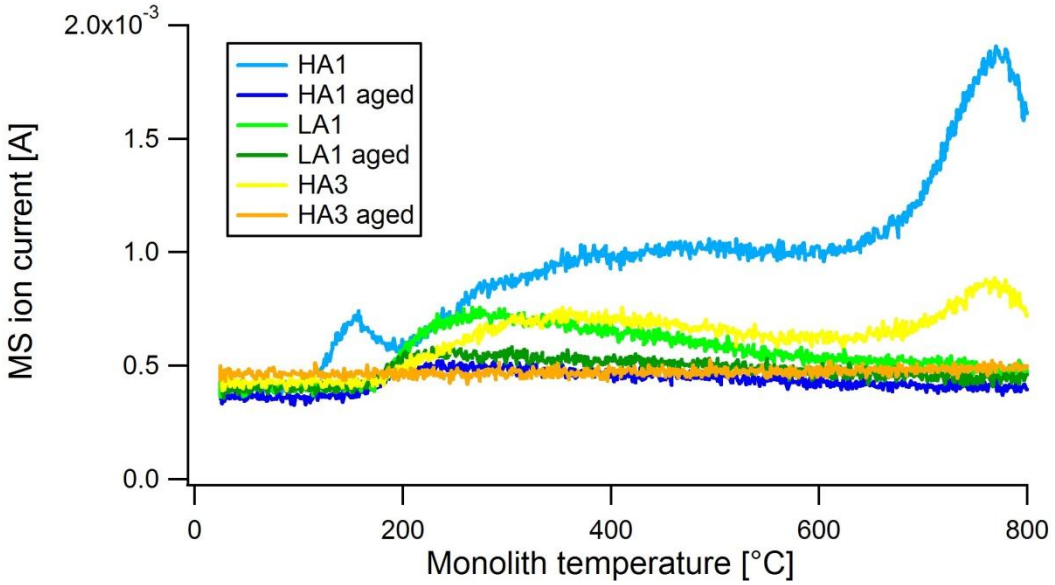

Figure 14: Desorption of H_2 from Pt/ceria monoliths during TPD. Flow: 50 ml/min, ramp rate: 20°C/min

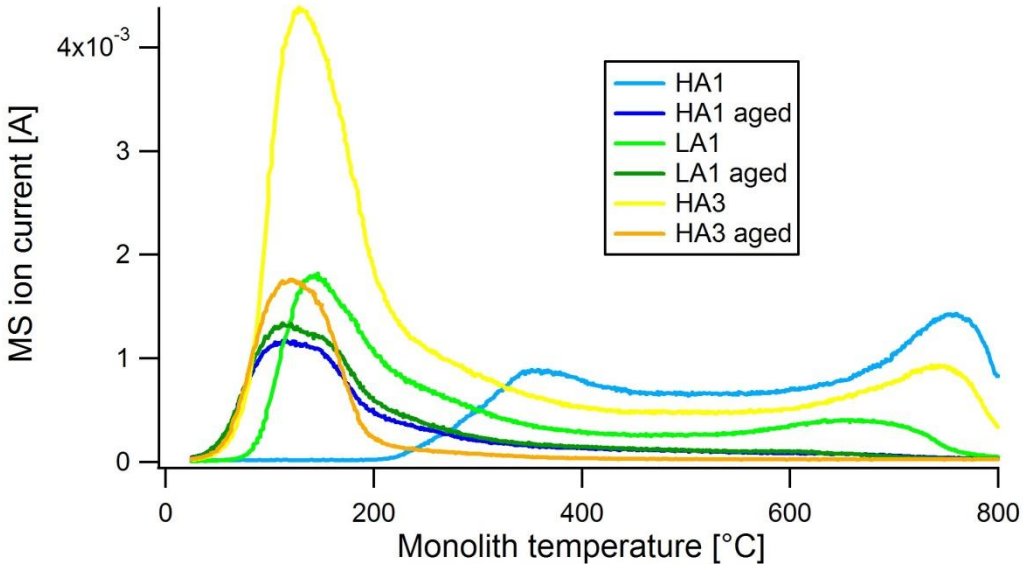

Figure 15: Desorption of CO_2 from Pt/ceria monoliths during TPD. Flow: 50 ml/min, ramp rate: 20°C/min.

Hydrogen desorption can only be observed from the fresh monoliths, preferably on the two high area samples. One distinctive desorption peak of CO_2 can be observed for all six samples at low temperature (ca. 150°C), while a second peak at higher temperatures (ca. 750°C) only can be observed for the fresh samples. Ageing shifts the lower desorption peaks (ca. 150°C) to even lower temperatures and the number of adsorbed molecules decrease.

4.2.3 Test of catalytic activity - CO oxidation

The CO conversion of the monolith samples shown in figure 16 and 17 was calculated from the CO_2 signal. Since the CO_2 level was higher than the CO level during oxidation, it was concluded that the CO_2-signal suffered from a smaller percentage of disturbance.

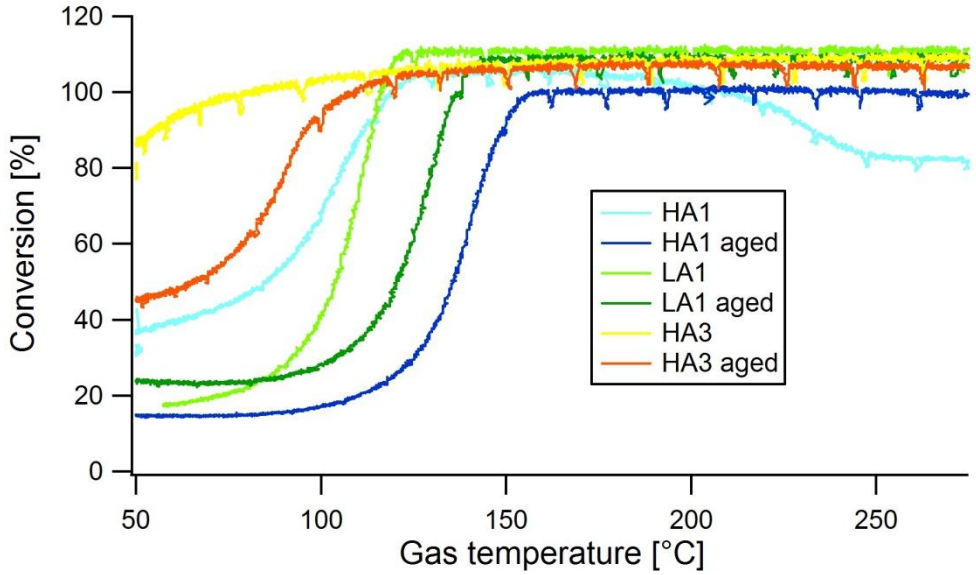

Figure 16: Conversion of CO during decreasing reactor temperature (extinction). Flow: 400 ml/min, ramp rate: 20°C/min.

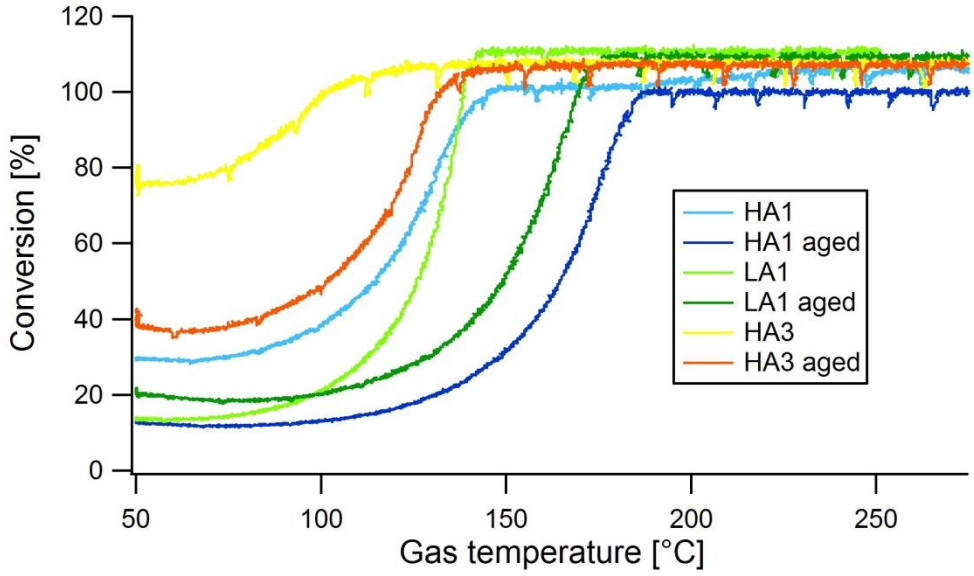

Figure 17: Conversion of CO during increasing reactor temperature (ignition). Flow: 400 ml/min, ramp rate: 20°C/min.

All of the prepared monolith catalysts show catalytic activity and exhibit high conversion for CO at T>200°C. The two samples containing the higher Pt-concentration, 3%, shows the highest conversions. The ageing treatment decreased the performance compared to the fresh samples and the activity is generally higher for a certain temperature during extinction compared to ignition.

The HA1 sample appears to be affected more by the ageing treatment compared to the LA1 sample. Both the extinction and ignition curves in figure 17 are shifted more towards higher temperatures for the HA1 aged sample compared to the LA1 aged sample.

4.2.4 Specific surface area of powder and monolith samples

The specific surface area (SSA) of the Pt/ceria powders before deposition on monoliths and can be seen in table 9 together with the initial SSA of the two types of ceria used. The SSA of the monoliths before and after measurements in the flow reactor can be seen in the table 10. The SSA was calculated with respect to the amount of washcoat, the empty monolith weigh was not included.

Table 9: Specific surface area of ceria and Pt/ceria powder.

Powder sample	SSA [m^2/g]
HA	250
LA	88.0
HA1	180
LA1	79.3
HA3	184

Table 10: Specific surface area of monolith samples before and after flow reactor measurement.

HA1 monolith		LA1 monolith		HA3 monolith	
SSA before [m^2/g]	SSA after [m^2/g]	SSA before [m^2/g]	SSA after [m^2/g]	SSA before [m^2/g]	SSA after [m^2/g]
167	46.8	89.4	61.1	153	59.3

The surface area for the monolith samples containing HA ceria was quite high before use, but it decreased greatly during the flow reactor experiments. The monolith with LA ceria possessed a lower original specific surface area compared the HA samples but do not sinter as severely during usage. All three samples end up with roughly the same specific surface area after use.

4.3 Diffuse reflectance infrared Fourier transform spectroscopy

Spectra for important steps of the two methods were extracted from the IR-data file and collected in a series of graphs for easier interpretation. A background, taken at 28 °C in argon after the pre-treatment was subtracted from each spectrum. The wavenumber range in the graphs was limited to 2500 – 100 cm^{-1} since this range contains the most interesting peaks.

According to a number of articles [25, 38, 39] the peak at ~2050 cm^{-1} represents CO linearly adsorbed on Pt while the peak at ~1800 cm^{-1} represents bridged CO on Pt. A peak corresponding to gas phase CO should be observed at slightly higher wavenumbers compared to CO on Pt [40]. The shoulder on the peak representing CO linearly adsorbed on Pt may originate from CO molecules being absorbed on Pt atoms with different coordination. It has been reported that peaks corresponding to CO on low coordinated Pt will be shifted to lower wavenumbers [38]. The twin peak at ~2300 cm^{-1} represents gas phase CO_2 [41, 40].

The large numbers of peaks observed in the range 1700 to 1000 cm^{-1} are much harder to assign but should according to literature originate from various carbonate species on the ceria support [42], e.g. hydrogen carbonate [43], monodentate and bidentate carbonate [44].These peaks also appear to overlap with the bridge-bonded CO at ~1800 cm^{-1}.

4.3.1 Measurements of dispersion

The IR-spectra collected for the CO/H_2/CO-method are shown in the following figures, figure 18 and figure 19.

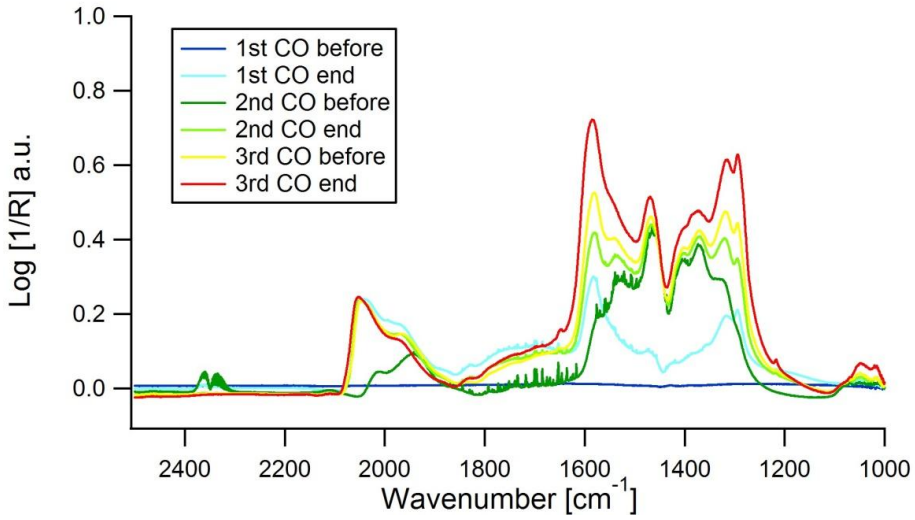

Figure 18: IR spectra obtained during the CO/H_2/CO-method performed on HA1 Pt powder.

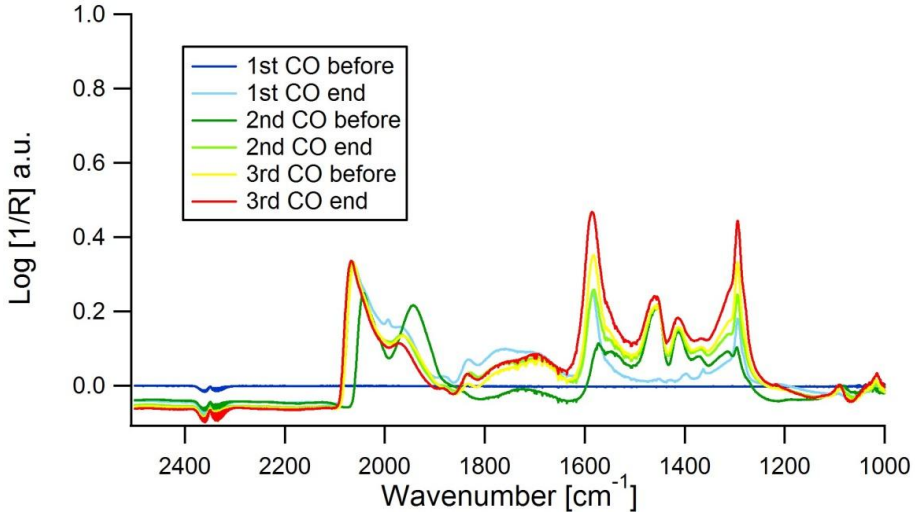

Figure 19: IR spectra obtained during the CO/H_2/CO-method performed on LA1 powder.

Similar spectra are obtained from both samples during the CO/H2/CO-methods. Peaks representing both CO on Pt and carbonate species on the support appear during the first CO-step. It appears that CO on Pt is partly removed by the reduction step between the 1st and 2nd CO-step. For the HA1 sample more CO is removed during this reduction compared to for the LA1 sample. However, the amount of carbonate species on the support does not decrease by this treatment. During the following CO-steps, peaks from CO on Pt as well as from carbonates on the support increase.

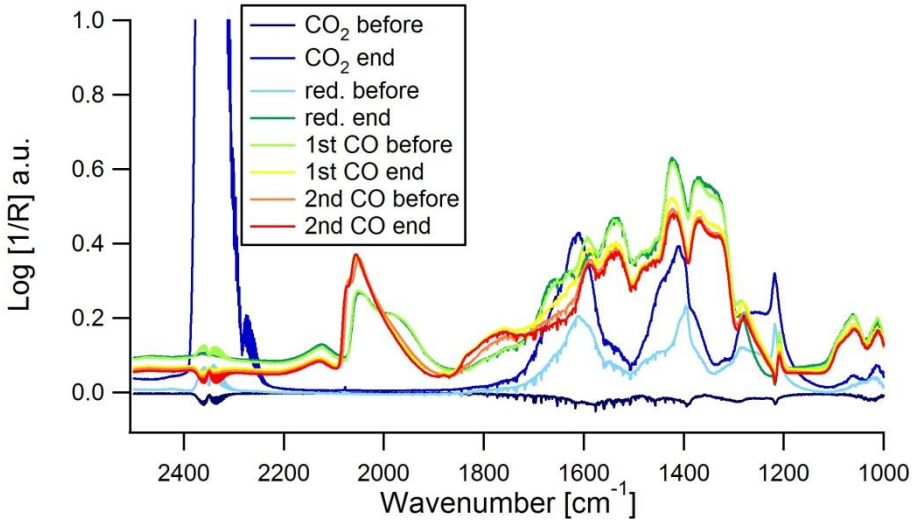

Figure 20: IR spectra obtained during the CO_2-method performed on HA1 powder.

The IR-spectra collected for the CO_2-method are shown figure 20. The supplied CO_2 is only stored as carbonates on the support, no peaks are visible in the area representing CO on Pt. However, after the reduction step, a peak corresponding to CO on Pt appears and many of the carbonate peaks increase. These peaks remain during the following CO-steps, CO linearly adsorbed on Pt slightly increase while the carbonate peaks slightly decrease.

4.3.2 Second pre-treatment

A second pre-treatment was performed after the $CO/H_2/CO$-measurement on the HA1 powder sample. IR spectra taken during the second pre-treatment can be found in figure 21. The first 25 minutes of the pre-treatment consist of a heating ramp from 28°C up to 400°C and the spectra obtained during this ramp are labelled with both time and temperature.

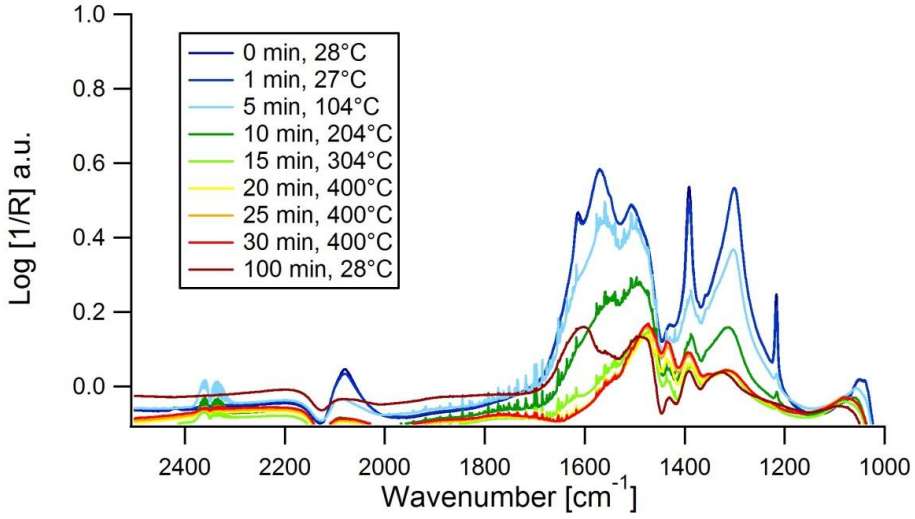

Figure 21: IR spectra obtained during the second pre-treatment performed on HA ceria + 1 wt.-% Pt powder.

Both carbonates on ceria and CO on Pt appear to be removed quite early as the temperature is raised. However, the spectra taken during elevated temperature are not entirely accurate since the background used was acquired at 28°C. The last spectrum shown is taken at 28°C at the end of the pre-treatment and implies that all CO on Pt is removed while some carbonates still remain.

5. Discussion

The aim of this master thesis project has been to acquire more knowledge about the Pt/CeO_2 system. As a starting point it was studied how the structure of the ceria support is affected by temperature and this will be evaluated first in the discussion.

Furthermore, two methods for measurements of platinum dispersion in Pt/CeO_2 catalysts were investigated using a flow-reactor equipment. These studies were complemented with DRIFTS to monitor the surface species formed during the different steps. The classical methods TPD and CO oxidation were also performed to further investigate the system.

Regarding heat treatments of the ceria powder, it can clearly be seen in figure 13 that the temperature is the single most important parameter under the conditions used here. Although, the surface area is lower after 17 h as compared to 2 h of heat treatment, this difference is minor. The change to a reducing environment does not cause more severe sintering at 300 or 400°C, but an effect can be seen at 500°C. At this temperature, the sample exposed to reducing environment for 3 h has a lower surface area compared the sample heated for 17 h in oxidizing environment.

One of the intentions of this part of the study was to investigate the maximum temperature which could be used during synthesis with as little impact as possible on the surface area. According to figure 13 and the result from the heat treatment in reducing atmosphere on Pt/ceria powder (section 4.1), temperatures below 400°C appears to have a minor impact on the surface area. Hence, the HA samples was kept above this temperature as little as possible during synthesis. Some exceptions had to be made to create stable catalyst: calcination of powder sample after impregnation (550°C, heat gradient and a hold of 15 min) and heat-gun pre-calcination of monoliths (600 °C, 1 min). The aim to avoid reduction of the surface area of the HA samples seems to have been achieved to some extent, since the SSA of the two HA monoliths were 153 and 166 m^2/g compared to only 89,4 m^2/g for the LA monolith. The low temperature approach was also applied during measurements in the flow reactor and the monoliths were not exposed to temperatures above 400°C until TPD and ageing. According the results in table 9, the largest decrease of the surface area occurs during impregnation with Pt since the SSA decrease from 250 m^2/g for pure HA ceria to approximately 180 m^2/g for HA1 and HA3.

The S-shape of the curves for samples in an oxidizing atmosphere implies that sintering mechanisms are depending on temperature. It is known that different mechanisms require different amount of energies in order to occur [45]. As the temperature is increased to above 400°C a significant decrease of the surface area is observed, probably because a certain sintering mechanism is inactive below this limit.

In figure 16 and 17 it can be observed that all catalysts investigated show catalytic activity and reaches high conversion for CO if the temperature is sufficient. The two samples containing the higher Pt-concentration, 3%, show the highest conversions. Since the CO-oxidation is strongly dependent on the Pt-surface this is not very surprising. All aged samples exhibit decreased activity compared to their fresh counterparts. This is as expected, since it was shown in the temperature study that subjecting a sample to 800°C for 2 h is sufficient to sinter the ceria support. Also, Pt is known to sinter at temperatures above 600°C if oxygen is present [46].

The capability of catalyzing oxidation of CO appears to decrease more for the HA1 sample compared to the LA1 sample during ageing treatment. The ignition and extinction curves for the aged HA1 is

more shifted toward higher temperatures compared to the aged LA1. The reason for this is most likely that HA1 has more Pt inside small pores of the support and these particles will be entirely blocked when the support sinter. For the LA sample, the small pores were likely already blocked during the pre-treatment of the ceria support at 800 °C before Pt was added. Hence, the Pt phase in the LA sample will not suffer from such severe blocking during the ageing in the flow reactor. Another explanation is that the Pt in the HA sample is more easily covered by mobilized support during ageing.

The HA1 sample exhibits lower conversion at T > 200 ° according to figure 16 and this is probably not accurate. It contradicts the common behaviour of catalysts (e.g. poisoning is unlikely at this temperature) and no other sample shows this behaviour. Since the extinction, a falling temperature gradient is the first part of the CO oxidation experiment; a likely cause is contamination of air in the CO and/or O_2 gas line.

Concerning the dispersion methods, both methods evaluated for measurement of noble metal dispersion in ceria containing systems show rather high repeatability. For the monoliths containing HA ceria, HA1 and HA3, the measurement of dispersion gave a lower value for the sample which had been subjected to ageing treatment. However the trends regarding the ageing treatment do not behave as could be expected for the LA1 sample. The dispersion appears to be higher *after* ageing treatment for this system. If indeed, the dispersion actually is measured this contradicts the usual behavior of the sintering mechanism, since elevated temperatures usually causes increased sintering. The CO-oxidation experiment shows that the LA1 sample loses catalytic activity after ageing which also contradicts an increased dispersion of Pt. It can clearly be seen in figure 16 and 17 that higher temperatures are needed after ageing to obtain a certain conversion level. Maybe the surface is able to reconstruct in some way that allows it to store more CO after the ageing treatment [8] or change the strength of absorption. However, by only looking at the dispersion values given by the chemisorption based methods is cannot be concluded if any of the methods work.

A high repeatability cannot alone prove the reliability of a certain method, i.e., prove that the involved steps fulfill the expected results. It is interesting to verify that the dispersion measurement methods evaluated function as the authors propose in their original papers. Here, the DRIFTS experiments were performed to study what happens on the surface during the gas treatments involved in the respective methods.

The CO/H_2/CO-method includes an intermediate reduction step between the CO pulses in order to obtain a clean platinum surface, while keeping the ceria covered with CO [5]. In the last part of the method, CO can be used as a probe since only the Pt surface should be available. The CO_2-poison method has a similar approach but utilizes a CO_2-pulse in combination with oxidizing and reducing steps to cover the ceria [25]. After these steps, only the ceria should be covered and subsequently, CO can be used as a probe on the Pt surface.

In the DRIFTS spectra for the HA1 powder sample undergoing CO/H_2/CO-measurement it can be seen that the reducing treatment between the first and second CO-pulse removes a lot of the CO from Pt, but not all as indented. The peak at 2050 cm^{-1} , representing CO on highly coordinated Pt, appears to diminish more compared the peak at ~2000 cm^{-1} corresponding to CO on lower coordinated Pt[38]. During the reducing step, the peaks from CO on Pt decreases while the peaks from the carbonates in the range 1700 – 1000 cm^{-1} increase, although no CO is added. It could be that the reduction causes a

migration of CO from the Pt to the support. This migration might be triggered by the encapsulation of Pt described by Bazin et al [38]. In their paper, they show that a reducing treatment at 500 °C can cause encapsulation of Pt particles by the support. This process is reversed by oxidation and does not occur at 200°C. The hydrogen is switched off at the same time as the temperature starts to decrease, i.e. the sample is subjected to an inert environment during cooling which might be sufficient to remove encapsulation. When the $CO/H_2/CO$ method is performed with the LA1 sample the reducing treatment seems to work even worse at removing CO on Pt. The behavior of the peak at 2500 cm^{-1} is similar to that of the HA1 sample, but the peak at 1950 cm^{-1} appears to increase instead of decrease. Overall, no significant decrease of adsorbed CO on Pt during the reduction step can be observed for this sample. During the following CO-steps, the bands corresponding to CO on Pt and carbonates on the support continue to grow.

The aim of the $CO/H_2/CO$ method was to use a reducing step after an initial CO step to obtain a clean Pt-surface while keeping the support blocked by CO. After this an ordinary chemisorption based approach with CO as probe molecule follows. The DRIFTS spectra indicate that this method does not work as intended, even though the method exhibits repeatability.

Neither does the aim of the CO_2-poison method appear to be achieved according to the DRIFTS spectra in figure 20. The CO_2 added is supposed to block only the support, but according to the spectra, CO appears on Pt after the reduction step and remains for the rest of the treatment. Also, the peaks corresponding to carbonates on the support increase during reduction. Maybe there is enough CO_2 left in gas phase during reduction that will be stored on the surface or maybe the increase originates from a spillover process where carbon species migrate from ceria to Pt. The authors based their method on DRIFTS measurement performed on ceria exposed to CO_2 or CO. The following figure is taken from their article:

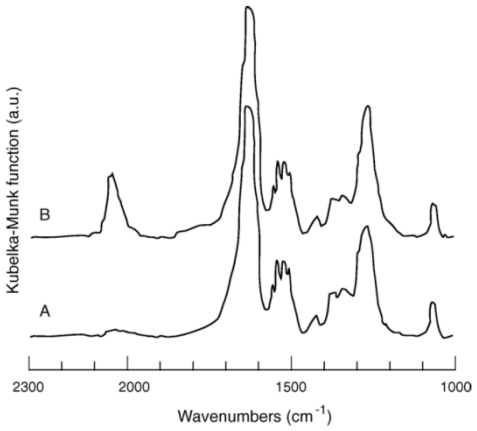

Figure 22: DRIFT spectra of CO adsorbed on 1 wt.% Pt/CeO_2 by the CO_2-poison method. (A) After CO_2 adsorption; (B) after CO adsorption [25].

As can be seen in spectrum (A), no Pt sites are filled during the CO_2-step. The authors assume that the Pt-sites are not filled until the CO-step as can be interpreted from spectrum (B). However, they do not follow what happens during the reduction step between the CO and CO_2-steps. According to our study, most of the Pt sites are already filled before CO is added. The authors of this article do not mention what type of ceria they use during their study, or what surface area it has. It might be that this method is better suited for ceria with a lower surface area compared to that used in this study (>50 m^2/g).

During the $CO/H_2/CO$ method, it appears to be very hard to saturate the support with carbon species. For both the HA and the LA sample, the bands representing the carbonates continue to grow through all three CO-steps. The total duration of these CO additions were 30+30+30 min, a considerable long time. The HA sample was left in the rector and subjected to a second pre-treatment, and it can be seen that right before the pre-treatment is started, the carbonate band are slightly lower compared to right after the last CO-pulse. It is possible that some bands correspond to physisorbed species that has not yet desorbed when the spectra was taken.

The peaks in the carbonate region of the spectra do not exhibit the same pattern after CO_2 adsorption as compared to after CO adsorption. This could be due to the uncertainty of the DRIFTS itself, or by actual differences of the material and method. Some ceria sites might not be able to incorporate carbonates from CO, only from CO_2. The carbonate peaks do not have the same shape during the CO_2-poison method as compared to during the $CO/H_2/CO$ method and the highest carbonate peaks are not obtained at the end of the CO_2-poison method, but rather after the reduction step. It should also be noted that after the reduction step in the CO_2-poison method, the carbonate peaks obtain an appearance more similar to the pattern in the spectra from the $CO/H_2/CO$ method.

The species released from the surface when the temperature was increased during TPD were CO_2, H_2 and some CO. The process taking place did not correspond to desorption based methods in a classical sense, since a reaction also was proceeding. The surface was not exposed to CO_2 and desorbed CO_2 probably originates from a reaction on the surface. CO could be oxidised on the Pt with oxygen supplied from ceria and adsorbed carbonates may decompose into CO_2. Another explanation is that CO can be oxidised by residual traces of water in the water gas-shift reaction, $CO + H_2O \rightarrow CO_2 + H_2$, as has been suggested by Foger and Andersen [47]. For high surface area supports, the residual water may be difficult to remove unless high temperatures area reached. This agrees well with the desorption peak appearing simultaneously at high temperatures for CO_2 and H_2, which can only be observed for fresh samples. This behaviour is not observed for the aged samples probably because the ageing at 800°C is sufficient to completely remove the adsorbed water. After the ageing treatment, CO_2 desorbs at a lower temperature, i.e. the peaks are shifted to the left. This could imply that the species do not adsorb as strongly after ageing due to re-construction of the surface.

By evaluation the spectra obtained during the second pre-treatment performed on the HA1 sample in the DRIFTS reactor, some qualitative information can be achieved about what surface species that are desorbed as CO_2. However, the heat treatment only reaches 400°C. The first CO_2 peak during TPD, 100-200°C, appears to originate both from CO on Pt as well as from the carbonate species on the support according to the DRIFTS spectra.

6. Future work

Further work is needed to understand catalyst systems with ceria-containing supports and a number of questions have arisen during this work.

More TPD studies in the DRIFTS equipment could help to understand the behaviour of the adsorbed carbonate species. The DRIFTS equipment could also be utilized to study if the support could be saturated with carbonates. If that is possible, the CO_2-poison method may work if the reduction step is excluded.

It should also be evaluated if there is a reduction treatment which is able to remove more CO from Pt compared to the 5 vol.-% H_2 at 300°C used during the $CO/H_2/CO$. Maybe the temperature needed will be too high for HA ceria but at least suitable for systems with lower surface area. It must be considered if this treatment can cause encapsulation as previously mentioned and also if it's possible to saturate the ceria with carbonates.

7. Conclusions

- Ceria is certainly a challenging system, and further studies are necessary.
- Pt/ceria catalysts exhibit high activity for CO oxidation at low temperature.
- Temperatures up to 400°C do not cause considerable sintering of the type of ceria support used in this study.
- Neither of the dispersion measurement methods evaluated behaves as expected according to complementary DRIFTS studies.
- Carbon-containing adsorbates on ceria are mainly released as CO_2.
- It takes very long time to saturate the ceria support with carbonates.
- The storage of carbon-containing adsorbate show different behaviour depending on if CO or CO_2 is supplied.
- CO_2 supplied at 28°C is only adsorbed on the ceria support, not on Pt.
- For LA ceria, it is harder to remove CO from Pt during reduction treatment compared to HA ceria.
- Repeatability does not imply a method measures as expected!

8. Acknowledgments

I would like to express my gratitude to everyone who have supported and helped me during my work with my master thesis. First of all, thank you Lisa Kylhammar for offering me this opportunity and for being an excellent mentor and supervisor. Also great thanks to my co-supervisor Per-Anders Carlsson for all the advice and inspiring discussions. Thanks to my examiner Magnus Skoglundh for keeping an eye on my proceedings and for having an open door for questions.

Thank you Anne Wendel for showing me the BET-equipment and Lars Lindström for all the help with fixing malfunctioning gas lines, Hanna Härelind-Ingelsten for introduction and support to the DRIFTS equipment and Ann Jakobsson for help with all practical things.

I would also like to thank all personnel and thesis workers in the division for creating a good atmosphere and for all help with everything from instruments to finding new house-hold paper. Especially I would like to thank all of my fellow room-mates.

Thanks to all you people in my bachelor programme, Maxi4Life and its incarnations for making five years at Chalmers feeling so short.

Finally, I would like to thank my family for always believing in me and my sister for helping me increasing the number of relatives undertaking higher education. It's nice that at least someone understands what I´ve been working with. And Victor, you've been the best the last couple of months. Thanks for everything.

References

1. Trovarelli, A., M. Boaro, et al. (2001). "Some recent developments in the characterization of ceria-based catalysts." Journal of Alloys and Compounds **323**: 584-591.
2. Zhou, H. P., H. S. Wu, et al. (2001). "Thermally Stable Pt/CeO2 Hetero-Nanocomposites with High Catalytic Activity." Journal of the American Chemical Society **132**(14): 4998 - 4999.
3. Becker, E., P. A. Carlsson, M. Skoglundh, (2009). "Methane Oxidation over Alumina and Ceria Supported Platinum." Topics in Catalysis **52**(13-20): 1957-1961.
4. Komai, S., Y. Yazawa, et al. (2005). "Determination of metal dispersion of Pt/CeO2 catalyst by CO-pulse method." Journal of the Japan Petroleum Institute **48**(3): 173-177.
5. Holmgren, A. and B. Andersson (1998). "Oxygen storage dynamics in Pt/CeO2/Al2O3 catalysts." Journal of Catalysis **178**(1): 14-25.
6. Teschner, D., A. Wootsch, et al. (2001). "Ceria as a new support of noble metal catalysts for hydrocarbon reactions: chemisorption and catalytic studies." Solid State Ionics **141**: 709-713.
7. Chorkendorff, I. , Niemantsverdriet, J. W., *Concepts of Modern Catalysis and Kinetics – Student Edition*, 2003, Wiley-VCH Verlag GmbH & Co, Weinheim, Germany, pp 1-11, 16-17, 183-188
8. Bowker, M., *The Basis and Applications of Heterogeneous Catalysis, 4th edition*, 1998, Oxford Science Publications, pp 1-28, 51-52, 56-62
9. Becker, E., *Interactions of methane and carbon monoxide with platinum – Supported catalysts and chemical sensors*, 2010, Chalmers Reproservice, Göteborg, Sweden, pp 13
10. *Various monoliths used in catalysis*, 2010-05-17, Available from: http://image.made-in-china.com/2f0j00HebQdgwnfqrp/Ceramic-Honeycomb-BHLJ-542-.jpg
11. Lin, W. Y., A. A. Herzing, et al. (2008). "Probing metal-support interactions under oxidizing and reducing conditions: in situ Raman and infrared spectroscopic and scanning transmission electron microscopic-X-ray energy-dispersive spectroscopic investigation of supported platinum catalysts." Journal of Physical Chemistry C **112**(15): 5942-5951.
12. Härelind Ingelsten, H. "Catalysis for Lean NO_X Reduction : aspects of catalyst synthesis and surface acidity", (2005), Chalmers reproservice, Göteborg, Sweden, pp 27-28
13. Niemansverdriet, J.W., Spectroscopy in Catalysis 2nd edition, (2000), Wiley VCH, Weinheim, Germany, pp 202-216
14. Azambre, B., O. Heintz, et al. (1999). "Optimization of some instrumental factors in diffuse reflectance infrared Fourier transform spectroscopy." Talanta **50**(2): 359-365.
15. Trovarelli "Catalysis by ceria and related materials", Imperial College Press, London, UK (2002), pp 15-24, figure pp 22
16. Mogensen, M., N. M. Sammes, et al. (2000). "Physical, chemical and electrochemical properties of pure and doped ceria." Solid State Ionics **129**(1-4): 63-94.
17. Kaspar, J., P. Fornasiero, et al. (1999). "Use of CeO2-based oxides in the three-way catalysis." Catalysis Today **50**(2): 285-298.
18. Tranquada, J. M., S. M. Heald, et al. (1989). "NATURE OF THE CHARGE-CARRIERS IN ELECTRON-DOPED COPPER-OXIDE SUPERCONDUCTORS." Nature **337**(6209): 720-721.
19. Butta, N., L. Cinquegrani, et al. (1992). "A FAMILY OF TIN OXIDE-BASED SENSORS WITH IMPROVED SELECTIVITY TO METHANE." Sensors and Actuators B-Chemical **6**(1-3): 253-256.
20. Weng, X. L., B. Perston, et al. (2009). "Synthesis and characterization of doped nano-sized ceria-zirconia solid solutions." Applied Catalysis B-Environmental **90**(3-4): 405-415.
21. Mikulova, J., J. Barbier, et al. (2007). "Wet air oxidation of acetic acid over platinum catalysts supported on cerium-based materials: Influence of metal and oxide crystallite size." Journal of Catalysis **251**(1): 172-181.
22. Gatica, J. M., R. T. Baker, et al. (2000). "Rhodium dispersion in a Rh/Ce0.68Zr0.32O2 catalyst investigated by HRTEM and H-2 chemisorption." Journal of Physical Chemistry B **104**(19): 4667-4672.
23. Acharya, C. K., A. M. Lane, et al. (2008). "Analysis of Gd level and Pt dispersion on ceria support for isobutane steam reforming." Catalysis Letters **121**(1-2): 12-18.
24. Tanabe, T., Y. Nagai, et al. (2009). "Low temperature CO pulse adsorption for the determination of Pt particle size in a Pt/cerium-based oxide catalyst." Applied Catalysis a-General **370**(1-2): 108-113.
25. Takeguchi, T., S. Manabe, et al. (2005). "Determination of dispersion of precious metals on CeO2-containing supports." Applied Catalysis a-General **293**: 91-96.

26. Papavasiliou, A., A. Tsetsekou, et al. (2009). "Development of a Ce-Zr-La modified Pt/gamma-Al2O3 TWCs' washcoat: Effect of synthesis procedure on catalytic behaviour and thermal durability." Applied Catalysis B-Environmental **90**(1-2): 162-174.
27. Duplan, J. L. and H. Praliaud (1991). "INFRARED DETERMINATION OF THE ACCESSIBLE METALLIC SURFACE OF SUPPORTED PALLADIUM CONTAINING CERIA." Applied Catalysis **67**(2): 325-335.
28. Pantu, P. and G. R. Gavalas (2002). "Methane partial oxidation on Pt/CeO2 and Pt/Al2O3 catalysts." Applied Catalysis a-General **223**(1-2): 253-260.
29. Rogemond, E., N. Essayem, et al. (1997). "Characterization of model three-way catalysts .1. Determination of the accessible metallic area by cyclohexane aromatization activity measurements." Journal of Catalysis **166**(2): 229-235.
30. Nagai, Y., K. Dohmae, et al. (2008). "In Situ Redispersion of Platinum Autoexhaust Catalysts: An On-Line Approach to Increasing Catalyst Lifetimes?" Angewandte Chemie-International Edition **47**(48): 9303-9306.
31. Nagai, Y., N. Takagi, et al. (2007). Real-time observation of platinum redispersion on ceria-based oxide by in-situ Turbo-XAS in fluorescence mode. X-Ray Absorption Fine Structure-XAFS13. B. Hedman and P. Painetta. **882:** 594-596.
32. Augustine , R. L., "Heterogeneous catalysis for the synthetic chemist", 1996, Marcel Dekker INC, New York, United States of America, pp 287-289
33. Dawody, J., M. Skoglundh, et al. (2005). "Role of Pt-precursor on the performance of Pt/BaCO3Al2O3-NOx storage catalysts." Journal of Molecular Catalysis a-Chemical **225**(2): 259-269.
34. Brunelle, J. P. (1978). "PREPARATION OF CATALYSTS BY METALLIC COMPLEX ADSORPTION ON MINERAL OXIDES." Pure and Applied Chemistry **50**(9-10): 1211-1229.
35. Harris, D. C., "Quantitative chemical analysis", 7th edition, 2007, W.H Freeman and Company, New York, United States of America, pp 478-488
36. *Main parts of a mass spectrometer*, 2010-05-18, Avaliable from: http://en.wikipedia.org/wiki/File:Ms_block_schematic.gif
37. Thomas, J. M.,W. J. Thomas, "Principles and practice of heterogeneous catalysis", (1997), VCH Verlagsgesellschaft mbH, Weinheim, Germany, pp 226-229
38. Bazin, P., O. Saur, et al. (2005). "FT-IR study of CO adsorption on Pt/CeO2: characterisation and structural rearrangement of small Pt particles." Physical Chemistry Chemical Physics **7**(1): 187-194
39. Primet, M., M. Elazhar, et al. (1990). "DETERMINATION OF THE ACCESSIBLE METALLIC SURFACE OF SUPPORTED PLATINUM - QUANTITATIVE INFRARED SPECTROSCOPIC STUDY OF CARBON-MONOXIDE ADSORPTION." Applied Catalysis **59**(1): 153-163.
40. Becker, E., P. Thormahlen, et al. (2007). "Low-temperature activity for CO oxidation over diesel oxidation catalysts studied by High Throughput Screening and DRIFT spectroscopy." Topics in Catalysis **42-43**(1-4): 421-424.
41. de Lima, S, A. da Silva, et al. (2010). "New approaches to improving catalyst stability over Pt/ceria during ethanol steam reforming: Sn addition and CO2 co-feeding. "Applied Catalysis B: Environmental **96**:387–398
42. Matsouka, V., M. Konsolakis, et al. (2008). "In situ DRIFTS study of the effect of structure (CeO2-La2O3) and surface (Na) modifiers on the catalytic and surface behaviour of Pt/gamma-Al2O3 catalyst under simulated exhaust conditions." Applied Catalysis B-Environmental 84(3-4): 715-722.
43. Jin, T., Y. Zhou, et al. (1987). "INFRARED AND X-RAY PHOTOELECTRON-SPECTROSCOPY STUDY OF CO AND CO2 ON PT/CEO2." Journal of Physical Chemistry **91**(23): 5931-5937.
44. Westerberg, B., FTIR Studies and Kinetic Modelling of NOx Reduction and NOx Storage, 2000, Chalmers reproservice, Göteborg, Sweden pp 17-19
45. Obradovic, N., S. Stevanovic, et al. (2009). "Influence of ZnO specific surface area on its sintering kinetics." Powder Metallurgy and Metal Ceramics **48**(3-4): 182-185.
46. Loof, P., B. Stenbom, et al. (1993). "RAPID SINTERING IN NO OF NANOMETER-SIZED PT PARTICLES ON GAMMA-AL2O3 OBSERVED BY CO TEMPERATURE-PROGRAMMED DESORPTION AND TRANSMISSION ELECTRON-MICROSCOPY." Journal of Catalysis **144**(1): 60-76.
47. Foger, K. and J. R. Anderson (1979). "TEMPERATURE PROGRAMMED DESORPTION OF CARBON-MONOXIDE ADSORBED ON SUPPORTED PLATINUM CATALYSTS." Applied Surface Science **2**(3): 335-351.

Appendix

A.1 Flow-reactor scripts

Table A-1. Script for the pre-treatment in flow-reactor.

Temp. [°C]	Gradient [°C/min]	Duration [min]	Gas	Gas conc.	Total flow [ml/min]	Comment
28	-	1	-	-	400	Ar
28-400	20	19	-	-	400	Ar + heating
400	-	5	-	-	400	S
400	-	20	O_2	5%	400	O_2 wash
400	-	10	-	-	400	Ar
400	-	20	H_2	5%	400	H_2 wash

Table A-2. Script for the CO/H_2/CO method in flow-reactor.

Temp. [°C]	Gradient [°C/min]	Duration [min]	Gas	Gas conc.	Total flow [ml/min]	Comment
400	-	-	-	-	400	Pre-treatment
400-28	20	19	-	-	400	Ar cool
28	-	221	-	-	400	S
28	-	60	CO	150ppm	400	1st CO-pulse
28	-	60	-	-	400	Ar
28-300	20	14	-	-	400	Ar + heating
300	-	46	-	-	400	S
300	-	20	H_2	5%	400	reduction
300-28	20	14	-	-	400	Ar cool
28	-	226	-	-	400	S
28	-	30	CO	150ppm	400	2nd CO-pulse
28	-	120	-	-	400	Ar
28	-	30	CO	150ppm	400	3rd CO-pulse
28	-	30	-	-	400	Ar

Table A-3. Script for the CO_2-poison method in flow-reactor.

Temp [°C]	Gradient [°C/min]	Time [min]	Gas	Gas conc.	Total flow [ml/min]	Comment
400	-		-	-	400	Pre-treatment
400-28	20	19	-	-	400	Ar cool
28	-	281	-	-	400	S
28	-	10	O_2	5%	400	O_2
28	-	10	CO_2	25%	400	CO_2-poison
28	-	5	-	-	400	Ar
28	-	10	H_2	5%	400	H_2
28	-	60	-	-	400	Ar
28	-	30	CO	150 ppm	400	1st CO-pulse
28	-	120	-	-	400	Ar
28	-	30	CO	150 ppm	400	2nd CO-pulse
28	-	30	-	-	400	Ar

Table A-4. Script for TPD in flow-reactor.

Temp. [°C]	Grad. [°C/min]	Duration [min]	Gas	Total flow [ml/min]	Comment
28	-	120	argon	50	
28-800	20	39	argon	50	Ar + heating
800	-	20	argon	50	
800-28	20	39	argon	50	
28	-	30	argon	50	

Table A-5. Script for CO oxidation in flow-reactor.

Temp. [°C]	Grad. [°C/min]	Duration [min]	Gas	Gas conc.	Total flow [ml/min]	Comment
400	-	-	-	-	400	Pre-treatment
400-300	20	5	-	-	400	Ar cool
300	-	30	-	-	400	S
300	-	20	CO/O_2	0.5% + 5%	400	ox. Start
300-50	2	125	CO/O_2	0.5% + 5%	400	extinction
50	-	60	CO/O_2	0.5% + 5%	400	S
50-300	2	125	CO/O_2	0.5% + 5%	400	ignition
300	-	30	-	-	400	S
300-28	20	19	-	-	400	Ar cool
28	-	30	-	-	400	Ar

A.2 DRIFTS scripts

Note: During the times in parenthesis, the system was allowed to stabilize before the IR-program was started and the gas program was changed immediately to the next step.

Table A-6. Script for the pre-treatment in DRIFTS-reactor.

Temp. [°C]	Gradient [°C/min]	Duration [min]	Gas	Gas conc.	Total flow [ml/min]	Comment
28	-	1	-	-	400	Ar
28-400	20	19	-	-	400	Ar + heating
400	-	5	-	-	400	S
400	-	20	O_2	5%	400	O_2 wash
400	-	5	-	-	400	Ar
400	-	20	H_2	5%	400	H_2 wash

Table A-7. Script for the CO/H_2/CO method in DRIFTS-reactor.

Temp. [°C]	Gradient [°C/min]	Duration [min]	Gas	Gas conc.	Total flow [ml/min]	Comment
400	-	-	-	-	400	Pre-treatment
400-28	20	5	-	-	400	Ar cool
28	-	(120)	-	-	400	S
28	-	30	CO	150ppm	400	1st CO-pulse
28	-	30	-	-	400	Ar
28-300	20	20	-	-	400	Ar + heating
300	-	10	-	-	400	S
300	-	20	H_2	5%	400	reduction
300-28	20	20	-	-	400	Ar cool
28	-	(120)	-	-	400	S
28	-	30	CO	150ppm	400	2nd CO-pulse
28	-	30	-	-	400	Ar
28	-	30	CO	150ppm	400	3rd CO-pulse
28	-	30	-	-	400	Ar

Table A-8. Script for the CO_2-poison method in DRIFTS-reactor.

Temp [°C]	Gradient [°C/min]	Time [min]	Gas	Gas conc.	Total flow [ml/min]	Comment
400	-		-	-	400	Pre-treatment
400-28	20	19	-	-	400	Ar cool
28	-	(120)	-	-	400	S
28	-	10	O_2	5%	400	O_2
28	-	10	CO_2	25%	400	CO_2-poison
28	-	20	-	-	400	Ar
28	-	10	H_2	5%	400	H_2
28	-	(120)	-	-	400	Ar
28	-	30	CO	150 ppm	400	1^{st} CO-pulse
28	-	30	-	-	400	Ar
28	-	30	CO	150 ppm	400	2^{nd} CO-pulse
28	-	30	-	-	400	Ar